AD-A089 853 NAVAL RESEARCH LAB WASHINGTON DC F/G 20/4
THE SENSITIVITY OF WAVE FORCE COMPUTATIONS TO COMMON ERRORS, UN--ETC(U)
SEP 80 S E RAMBERG, J M NIEDZWECKI
UNCLASSIFIED NRL-MR-4206 NL

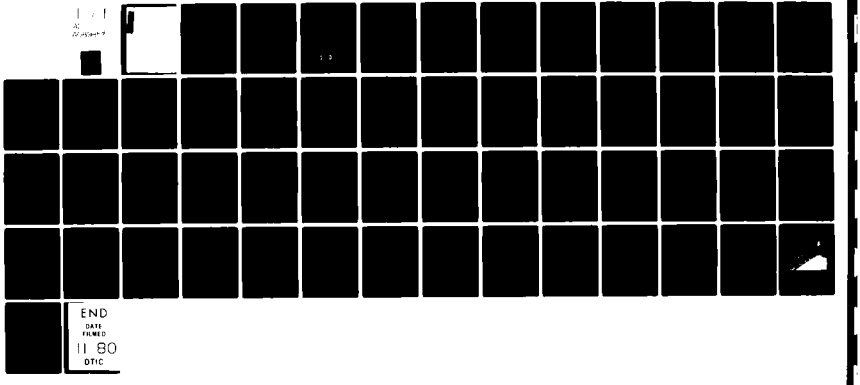

END
DATE FILMED
11 80
DTIC

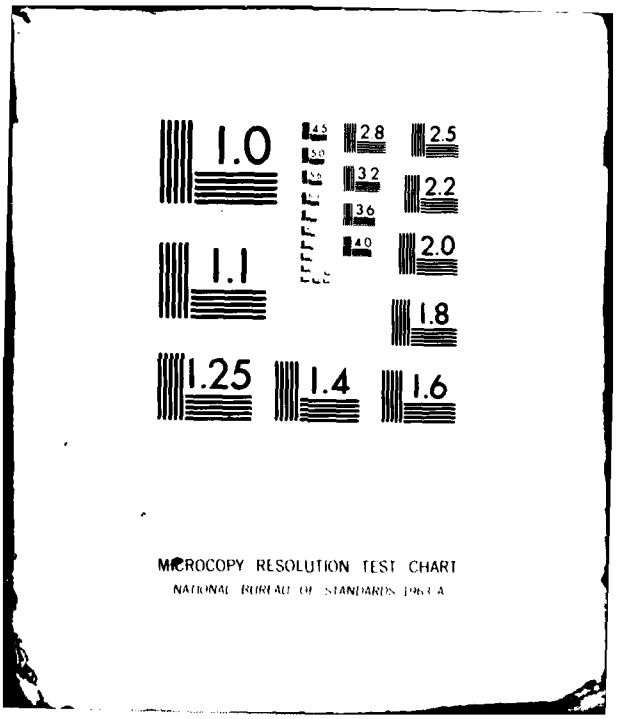
1.0
1.1
1.25
1.4
1.6
1.8
2.0
2.2
2.5
2.8
3.2
3.6
4.0
MICROCOPY RESOLUTION TEST CHART
NATIONAL BUREAU OF STANDARDS 1963-A

(14) NRL-MR-4206

SECURITY CLASSIFICATION OF THIS PAGE (When Data Entered)

(9) **REPORT DOCUMENTATION PAGE**

READ INSTRUCTIONS BEFORE COMPLETING FORM

1. REPORT NUMBER: NRL Memorandum Report 4206	2. GOVT ACCESSION NO.: AD-A089853
3. RECIPIENT'S CATALOG NUMBER:	
4. TITLE (and Subtitle): (6) THE SENSITIVITY OF WAVE FORCE COMPUTATIONS TO COMMON ERRORS, UNCERTAINTIES, AND HYDRODYNAMIC APPROXIMATIONS	5. TYPE OF REPORT & PERIOD COVERED: Interim report on a continuing problem
	6. PERFORMING ORG. REPORT NUMBER:
7. AUTHOR(s): (10) Steven E. Ramberg and John M. Niedzwecki	8. CONTRACT OR GRANT NUMBER(s): (17)
9. PERFORMING ORGANIZATION NAME AND ADDRESS: Naval Research Laboratory, Washington, D.C. 20375	10. PROGRAM ELEMENT, PROJECT, TASK AREA & WORK UNIT NUMBERS: 61153N RR0230141 84-0273-0-0
11. CONTROLLING OFFICE NAME AND ADDRESS: (11) Office of Naval Research, Washington, D.C.	12. REPORT DATE: 10 Sept[illegible] 1980
	13. NUMBER OF PAGES: 54
14. MONITORING AGENCY NAME & ADDRESS (if different from Controlling Office): (14) RR[illegible] 01 (12) 55	15. SECURITY CLASS. (of this report): Unclassified
	15a. DECLASSIFICATION/DOWNGRADING SCHEDULE:

16. DISTRIBUTION STATEMENT (of this Report)

Approved for public release; distribution unlimited.

17. DISTRIBUTION STATEMENT (of the abstract entered in Block 20, if different from Report)

18. SUPPLEMENTARY NOTES

19. KEY WORDS (Continue on reverse side if necessary and identify by block number)

Wave forces
Unsteady fluid forces
Vortex wakes
Offshore structures
Morison equation

20. ABSTRACT (Continue on reverse side if necessary and identify by block number)

The present investigation examines the methods and the hydrodynamic approximations commonly employed in wave force analysis. Alternatives and modifications are sought which improve the resolution of a general Morison approach. This is accomplished by considering two basic arrangements; a vertical cylinder and a horizontal cylinder in progressive waves. The physical differences between the flows are explored and the results are compared to previous planar harmonic flow measurements.

(Continued)

DD FORM 1 JAN 73 1473 EDITION OF 1 NOV 65 IS OBSOLETE
S/N 0102-014-6601

SECURITY CLASSIFICATION OF THIS PAGE (When Data Entered)

251950

20. ABSTRACT (Continued):

It was found that modifications to the usual Morison approach are required to adequately account for the orbital motions of the fluid and to account for the orientation of the orbits with respect to the cylinder axis. The consequences of these findings are discussed for inclined cylinders in waves and for cylinders in short-crested seas. The axial variations of the wave force on vertical cylinders are examined in order to establish error bounds for the common practice of assuming constant values of C_M and C_D over the entire span. Also, the methods of computing force transfer coefficients from a force record are examined and errors of method are identified and briefly discussed.

CONTENTS

THE SENSITIVITY OF WAVE FORCE COMPUTATIONS TO COMMON ERRORS, UNCERTAINTIES, AND HYDRODYNAMIC APPROXIMATIONS

1.0 INTRODUCTION

In the face of rising construction costs, the increased importance of dynamic loadings, and in view of the more hostile sites under consideration, the accuracy of wave force computations becomes a critical question. The least well understood wave loading regime, hence the one with the least accurate descriptions, is the regime wherein both drag and inertia forces are important. The basis for most wave force computations in this regime is the so-called Morison equation. In the past the Morison approach has been tailored with some success to particular applications. However attempts to generalize the approach have not been successful and as a consequence, large uncertainties can accompany a new application. The discrepancies between prediction and observation are often as large as 50 to 100 percent [1].

For the most part these inaccuracies stem from a poor understanding of the unsteady vortex flows which occur in this regime and from several simplifications inherent in the usual Morison approach. In lieu of a complete hydrodynamic description of the complex vortex wake flows, an unlikely accomplishment in the near future, an improved approach to wave force prediction appears to be one that can account for the major differences between wake flows which may occur for various wave-cylinder combinations. This report outlines such an approach and at the same time identifies uncertainties that can arise from differences in the methods of force or force coefficient calculation.

Manuscript submitted February 20, 1980.

Most investigations of the fluid forces on an object immersed in an unsteady flow begin by resolving the force into drag and inertia components [2]. It is less widely known that the general unsteady force also contains a history term and should be written as the sum of three contributions in the form,

$$F_{Total}(t) = F_{Drag}(u) + F_{Inertia}(\dot{u}) + F_{History}(u,\ \dot{u},\ t) \tag{1.1}$$

where u and $\dot{u}$ are the velocity and acceleration, respectively, which depend only on the time t. Some years ago, Morison et al [3] made use of this approach in attempting to describe the wave forces on a cylinder. In essence, they took an elemental force on the cylinder to be of the form

$$dF(t,s) = dF_{Drag} + dF_{Inertia} \tag{1.2}$$

where

$$dF_{Drag} = 1/2\,\rho\ D\ C_D\ u|u|ds \tag{1.3}$$

and

$$dF_{Inertia} = \pi/4\,\rho\ D^2\ C_M\ \dot{u}\ ds \tag{1.4}$$

and with s measured along the cylinder axis. Since this equation first appeared it has become the basis for the majority of practical wave force computations and is widely known as the Morison equation. The unknown force transfer coefficients C_M and C_D are usually taken as time invariants so that the unsteadiness of the force resides entirely in the variations of u and $\dot{u}$.

Along with the recent growth of offshore construction, considerable effort has been expended to collect values of C_M and C_D and to correlate the changes in the coefficients with the important parameters of the problem. Except for a few simple cases, notably not including progressive wave flows, the variations in the force transfer coefficients have not been completely accounted for. To be sure, one can obtain reasonably good force estimates but even with great care in the analysis errors of 20 to 50 percent in the total force are common and errors in the local force are often as great as 100 percent or more [1].

The objective of the present investigation is to improve the resolution of the Morison approach by first examining the sensitivity of the computed wave forces (or computed coefficients) to the common simplifications of method and to the common hydrodynamic approximations. Then, alternatives or modifications that can improve the resolution are considered. These are compared to wave force data obtained in a laboratory channel and are compared to previous results for simple oscillatory flows about cylinders [4, 5, 6, 7, 8]. By way of example, the present approach can be introduced by considering a simplification of method and a hydrodynamic approximation that already have occurred in passing from Eq. 1.1 to Eq. 1.2.

The simplification is due to the apparent lack of a history term in Morison's equation as compared to the general Eq. 1.1. However, if the flow is purely periodic ($\theta = \omega t$) the omission does not actually occur because the now periodic history term is included in the periodic drag and inertia terms. This can be demonstrated as follows. Let the drag and inertia forces be written in the usual way

$$dF_{Drag} \sim C_D^* \, u|u| ds \tag{1.5}$$

and

$$dF_{Inertia} \sim C_M^* \, \dot{u} \, ds. \tag{1.6}$$

With little or no loss in generality the *periodic* history term can be expanded in the form

$$dF_{History} = (1/2 \, \rho \, D \, C_{DH}^* \, u|u| + \pi/4 \, \rho \, D^2 C_{MH}^* \, \dot{u}) \, ds \tag{1.7}$$

because both u and $\dot{u}$ will be composed of orthogonal periodic functions. One can then redefine coefficients to obtain

$$dF(\theta) = (1/2 \, \rho \, D \, C_D \, u|u| + \pi/4 \, \rho \, D^2 \, C_M \, \dot{u}) \, ds \tag{1.8}$$

where

$$C_D = C_D^* + C_{DH}^* \tag{1.9a}$$

and

$$C_M = C_M^* + C_{MH}^* \tag{1.9b}$$

represent *composite* force transfer coefficients. The significance of this simplification is that the composite coefficients obtained from either of two separate experiments may not be appropriate when the two flows are superimposed. Important problems in this category are the forces on a structure exposed to a wave/current system or one experiencing oscillatory motion as well. The history term will not be considered further in this investigation; here the coefficients C_M and C_D represent composite values for nominally purely periodic flows.

The hydrodynamic approximation in Eq. 1.2 is the assumption that Eq. 1.1 can be extended to two-dimensional flows by taking a differential approach and then assuming that the distributed force depends only on the local kinematics of the flow. In fact, the variation of flow along the span will introduce three-dimensional effects in a number of ways. The axial pressure gradient will produce an axial component of velocity which can greatly influence wake formation. Less obvious is the effect arising from the wake which may be swept back over one segment of the structure after being generated at another segment under different flow conditions. Three-dimensional effects have been observed to have a pronounced influence on the drag in steady bluff body flows [15,16]. This approximation is examined further in Section 3.0 of this report along with other sources of errors and uncertainties. Before these are considered a brief review of previous results from planar or one-dimensional harmonic flows is presented.

2.0 SIMPLE OSCILLATORY FLOWS – A REVIEW OF RESULTS AND METHODS

The experiments of Sarpkaya [4, 5], Bearman et al. [6, 7], Maull and Milliner [8], and to a slightly lesser extent the experiments of Keulegan & Carpenter [9] belong in the category of simple oscillating flows over a cylinder. Each investigation approaches the conditions for which Eq. 1.1 is written and therefore does not require several of the usual assumptions and

simplifications of Morison's equation necessary for wave flows. Most importantly, each flow is one-dimensional or nearly so.

Sarpkaya's cylinders were mounted in the horizontal section of a large, U-tube apparatus. A similar arrangement was used by Maull and Milliner [8] and Bearman et al. [6,7]. Once set in motion, the fluid oscillated back and forth over the cylinder at the natural period of the water column. Keulegan & Carpenter placed their cylinders horizontally under the node of a standing wave. In all of these studies the fluid velocity and acceleration fields could be adequately described by the single components

$$u = U_m \cos\theta \tag{2.1a}$$

and

$$\dot{u} = -\frac{2\pi}{T} U_m \sin\theta. \tag{2.1b}$$

In each case the flow did not vary along the cylinder axis and Eq. 1.8 could be directly integrated over the cylinder length L to obtain

$$F(\theta) = 1/2\,\rho\, D\, C_D\, L\, U_M^2 \cos\theta|\cos\theta| - \pi^2/2T\rho\, D^2\, L\, C_M\, U_M \sin\theta \tag{2.2}$$

for the total unsteady force. By matching this expression with the experimental results it has been found that the variations in C_D and C_M could be accounted for through the use of any two of the following three parameters.

$$\frac{U_m T}{D} \equiv \text{period parameter} \equiv K \text{ (Keulegan-Carpenter number)} \tag{2.3a}$$

$$\frac{U_m D}{\nu} \equiv \text{Reynolds numbers} \equiv R \tag{2.3b}$$

$$\frac{D^2}{\nu T} \equiv \text{frequency parameter} \equiv \beta \tag{2.3c}$$

Only two of the three parameters are independent because $R = \beta \cdot K$. The period parameter and Reynolds number are often emphasized because of the analogy with inverse Strouhal number and Reynolds number in steady flows. Unfortunately both K and R contain U_m and this can mask important frequency effects. The use of the frequency parameter β has a certain practical advantage since it is a constant for a given wave/cylinder combination.

Using the Keulegan-Carpenter number, the above equation for the fluid force may be written in the non-dimensional form

$$f(\theta) = \frac{F(\theta)}{1/2\,\rho\,D\,L\,U^2} = C_D \cos\theta|\cos\theta| - \frac{\pi^2}{K} C_M \sin\theta, \tag{2.4}$$

which will be employed in the balance of this investigation. In this form it is also readily apparent that the ratio of the peak drag force to the peak inertia force is given by $C_D K/\pi^2 C_M$ and this should be kept in mind when assessing the relative importance of errors in C_M and C_D for various ranges of K. The conclusions that have been drawn from the one-dimensional or planar-flow experiments are:

i) Morison's equation **appears** to adequately describe the in-line force for simple one-dimensional oscillating flows about *circular* cylinders.

ii) Tabulations of C_M and C_D are available for predicting in-line fluid forces on circular cylinders in one-dimensional oscillating flows; see Figures 1 and 2.

iii) Several shortcomings in the Morison approach have been identified for non-circular, sharp-edged cylinders [6, 7].

iv) Large cycle-to-cycle variations in C_M and C_D can occur even for nearly uniform total forces as measured by the root-mean-square (rms) value [6, 7, 8].

v) A side or lift force is generated which may be nearly as large as the in-line force [9,10].

As stated in the introduction, the direct application of these results to wave force prediction has resulted in large errors. This is not surprising in view of the added complexities of wave-induced flows but it suggests certain objectives. For example, one could decide to retain the usual form of Morison's equation and then catalog values of C_M and C_D for each different

situation. This is the pragmatic approach taken by much of the offshore industry and will, or course, pose some difficulty for every new situation. Alternatively one could modify the equation in search of forms that permit a single tabulation or several tabulations of C_M and C_D to certain levels of accuracy and equation complexity. Both approaches are examined in the following sections, but first it is instructive to present the three common methods for determining C_M and C_D from a force record.

The first method makes use of the fact that the drag force is a maximum when the inertia force is zero ($\theta = 0, \pi$) and vice versa ($\theta = \pi/2,\ 3\pi/2$). The measured force is then examined at these special times in the cycle and set equal to either the drag or inertia force as appropriate. This method is very simple and has the added advantage of relying primarily on peak forces. However, it lacks averaging to cancel spurious errors, and in more complex flows the presence of harmonics can distort the results (see section 3.1). Morison et al [3] used this approach but with the advent of digital computers to handle the data reduction single-point methods have largely been abandoned.

The second method employs a Fourier analysis of the force coefficients. Let the nondimensional, measured force be given by Eq. 2.4, and then multiply it by $\sin\theta$ and integrate over a cycle. This yields the inertia coefficient

$$C_M \equiv \frac{\int_o^{2\pi} f_{meas}(\theta)\,\sin\theta\ d\theta}{\frac{\pi^2}{K}\int_o^{2\pi}\sin^2\theta} = -\frac{K}{\pi^3}\int_o^{2\pi} f_{meas}\,\sin\theta\ d\theta. \tag{2.5}$$

When the measured force is multiplied by $\cos\theta$ and integrated over a cycle, the drag coefficient is given by

$$C_D = \frac{\int_o^{2\pi} f_{meas}(\theta)\,\cos\theta\ d\theta}{\int_o^{2\pi}\cos^2\theta|\cos\theta|\,d\theta} = \frac{3}{2}\int_o^{2\pi} f_{meas}\,\cos\theta\ d\theta \tag{2.6}$$

The integrals can be evaluated numerically using the measured force. The Fourier approach emphasizes the periodic nature of the problem and can be extended to find any desired harmonic in the measured force record as was done originally by Keulegan & Carpenter.

The third method is a least-squares curvefit[1] given by the weighted sum of the squares of the force residuals,

$$S = \sum_{i=1}^{N} W_i [f_{meas} - f(\theta)]_i^2 \tag{2.7}$$

subject to the constraints

$$\frac{\partial S}{\partial C_M} = \frac{\partial S}{\partial C_D} = 0. \tag{2.8}$$

This will minimize the differences between the measured and calculated forces in the least-square sense. Performing the differentiation for the general coefficient C gives

$$\frac{\partial S}{\partial C} = \frac{\partial}{\partial C} \Sigma\ W_i [f_{meas}^2 - 2\, f_{meas}\, f(\theta) + f^2(\theta)]_i = 0 \tag{2.9}$$

or

$$\Sigma\, W_i \left[\frac{\partial f_{meas}^2}{\partial C} - 2\, f_{meas}\, \frac{\partial f(\theta)}{\partial C} + 2 f(\theta)\, \frac{\partial f(\theta)}{\partial C} \right]_i = 0 \tag{2.10}$$

and

$$\Sigma\ W_i\, f_{meas_i}\, \frac{\partial f(\theta_i)}{\partial C} = \Sigma\ w_{f_i}\, f(\theta_i)\, \frac{\partial f(\theta_i)}{\partial C}. \tag{2.11}$$

where the summation is understood to be over the N data points.

Introducing Eq. 2.4, to get

$$\frac{\partial f_i}{\partial C_D} = \cos\theta_i |\cos\theta_i| \tag{2.12}$$

and

$$\frac{\partial f_i}{\partial C_M} = -\frac{\pi^2}{K} \sin\theta_i \tag{2.13}$$

[1]See Appendix A for a description of the least-squares method.

yields two equations

$$C_D = \frac{\Sigma\ W_i\ f_{meas_i} \cos\theta_i |\cos\theta_i|}{\Sigma\ W_i \cos^4\theta_i} + \left[\frac{\pi^2}{K}\ C_M\right] \frac{\Sigma\ W_i \cos\theta_i |\cos\theta_i| \sin\theta_i}{\Sigma\ W_i \cos^4\theta_i} \tag{2.14}$$

and

$$C_M = \frac{\Sigma\ W_i\ f_{meas_i} \sin\theta_i}{\frac{\pi^2}{K} \Sigma\ W_i \sin^2\theta_i} + C_D \frac{\Sigma\ W_i \cos\theta_i |\cos\theta_i| \sin\theta_i}{\frac{\pi^2}{K} \Sigma\ W_i \sin^2\theta_i} \tag{2.15}$$

which can be solved for C_M and C_D. Clearly, if the quantity $\Sigma\ W_i \cos\theta_i\ |\cos\theta_i| \sin\theta_i$ is zero then the solutions for C_M and C_D are given by the first terms of Eqs. 2.14 and 2.15. For uniform statistical weighting (W_i = constant) and for equal increments in θ_i from 0 to 2π inclusive, this quantity is identically zero and the solutions for C_D and C_M reduce to

$$C_D = \frac{\Sigma\ f_{meas_i} \cos\theta_i |\cos\theta_i|}{\Sigma \cos^4\theta_i} \tag{2.16}$$

and

$$C_M = -\frac{K}{\pi^2} \frac{\Sigma\ f_{meas_i} \sin\theta_i}{\Sigma \sin^2\theta_i}. \tag{2.17}$$

Analogous equations can be obtained using an integral error criterion[2] with the results

$$C_D = \frac{4}{3\pi} \int_o^{2\pi} f_{meas} \cos\theta |\cos\theta|\, d\theta \tag{2.18}$$

and

$$C_M = -\frac{K}{\pi^3} \int_o^{2\pi} f_{meas} \sin\theta\ d\theta \tag{2.19}$$

which were utilized by Sarpkaya [5]. The advantage of the integral formulation is that the terms containing $\cos\theta|\cos\theta|\sin\theta$ drop out during the integration, but it must be employed with some caution because f_{meas} is usually a discrete function and the integral criterion becomes strictly inappropriate. Under the conditions set forth in Appendix A the integral and discrete least-squares method can be used interchangeably. Those conditions are tantamount to the

[2]See Appendix A.

conditions imposed above to make the discrete summations of $\cos\theta|\cos\theta|\sin\theta$ vanish and require the integrals to be evaluated in a certain way as well.

Upon comparing the integral least-squares results and the Fourier results the expressions for C_M are found to be identical but the two methods produce different equations for C_D. This difference can be examined by first supposing that the measured fluid drag force is proportional to $\cos\theta|\cos\theta|$. For this condition the two methods produce the same numerical result as they should. On the other hand a drag force proportional to $\cos\theta$ or proportional to $\cos^3\theta$ will produce about a 4 percent difference between computed coefficients. Sarpkaya applied both methods to his measured forces and found a small but consistent difference between results which, according to the above, would imply the presence of large even harmonics of the force *other* than those due to $\cos|\cos\theta|$. In other words, Morison's equation may not account for all of the significant in-line forces even for a simple planar flow.

If, for some reason, the statistical weighting is not uniform or a few irregular intervals in θ_i are chosen, then the full Eqs. 2.14 and 2.15 must be solved. To do this we first make the following substitutions

$$f_M = f_{meas} \tag{2.20a}$$

$$f_I = \frac{\pi^2}{K}\sin\theta_i \tag{2.20b}$$

$$f_D = \cos\theta_i|\cos\theta_i| \tag{2.20c}$$

in Eqs. 2.14 and 2.15 to get

$$C_D = \frac{\Sigma W_i f_M f_D}{\Sigma W_i f_D^2} + C_M \frac{\Sigma W_i f_D f_I}{\Sigma W_i f_D^2} \tag{2.21}$$

and

$$C_M = \frac{-\Sigma W_i f_M f_I}{\Sigma W_i f_I^2} + C_D \frac{\Sigma W_i f_D f_I}{\Sigma W_i f_I^2}. \tag{2.22}$$

The solutions for the coefficients are

$$C_D = \frac{\Sigma\, W_i\, f_M\, f_D \cdot \Sigma\, W\, f_I^2 - \Sigma\, W_i\, f_I\, f_D\, \Sigma\, W_i\, f_I\, f_M}{\Sigma\, W_i\, f_I^2 \cdot \Sigma\, W\, f_D^2 - (\Sigma\, W_i\, f_I\, f_D)^2} \tag{2.23}$$

and

$$C_M = \frac{-\Sigma\, W_i\, f_M\, f_I \cdot \Sigma\, W\, f_D^2 + \Sigma\, W_i\, f_I\, f_D}{\Sigma\, W_i\, f_I^2 \cdot \Sigma\, W\, f_D^2 - (\Sigma\, W_i\, f_I\, f_D)^2} \tag{2.24}$$

These equations are of the form given by Chakrabarti et al [10, 11] in their studies of wave forces on inclined cylinders. The sign changes in Eq. 2.24 as compared to Chakrabarti's expression are a consequence of the minus sign before the inertia term in Eq. 2.2 which is in turn a result of the definitions in Eq. 2.1.

One important source of error which is common to all of the above methods is that due to an uncertainty in the phase between the fluid motion cycle and the measured force cycle. This uncertainty can arise from a phase shift in some portion of the sensing or signal processing systems or may occur physically as a result of cycle-to-cycle variations in the wake processes. Whatever the cause, the sensitivities of the usual Morison coefficients to an arbitrary phase shift are given by

$$C_M'/C_M = \frac{8\pi\, C_D}{3K\, C_M} \sin\phi + \cos\phi \tag{2.25}$$

and

$$C_D'/C_D = I(\phi) - \frac{32K\, C_M}{9\pi^2\, C_D} \sin\phi \tag{2.26}$$

when the measured force is assumed to be given by Morison's equation but phase-shifted in the integral least-square expressions by an amount ϕ. The primes in the numerators are used to denote the phase-shifted coefficients as compared to the "correct" values in the denominators and on the right-hand sides. The term denoted by $I(\phi)$ is a lengthy trigonometric expression which is closely approximated by $\cos\phi$ for the present purposes. Two features, which are

expected, become apparent and quantified in these expressions. First is the tendency to swap one component for the other as the phase shifts [1] and the second is the marked influence of the quantity $\frac{\pi^2}{K}\frac{C_D}{C_M}$ which is the ratio of peak drag force to peak inertia force as discussed in connection with Eq. 2.4. These equations are plotted in Figure 3 for several values of the phase shift ϕ. In viewing the figure it must be kept in mind that large errors in either C_M or C_D are relatively unimportant when the *other* force component dominates the total force as determined by the ratio $\frac{\pi^2}{K}\frac{C_D}{C_M}$. The most striking results in the figures are the significant errors (5-10 percent) which can occur for phase shifts as small as 1 or 2 percent of the cycle. Clearly, special care must be taken to remove or identify phase shifts in the measurement system.

Before considering wave flows one further comment is in order. Experiments with simple oscillatory flows as described here have revealed the presence of large transverse or side forces that are not accounted for in the Morison equation. The side or lift force as it is sometimes called arises from the asymmetric vortex shedding that occurs for moderate and large Keulegan-Carpenter numbers. If K is large enough, the transverse force can oscillate a number of times during a wave cycle in relation to the number of vortices shed. This not only raises the possibility of flow-induced vibrations but also raises the possibility that the resultant peak force on the cylinder will be *greater* than the peak force predicted by Morison's equation. Maximum side forces of comparable magnitude to the maximum in-line force have been recorded in one-dimensional experiments. This difficulty may not be as severe in wave flows because the three-dimensional character of such flows tends to limit the spanwise coherence of the shedding processes. It should be noted, however, that cylinder vibrations can restore the coherence and therefore deserve consideration.

3.0 WAVE FLOW APPROXIMATIONS AND UNCERTAINTIES

The velocity and acceleration fields induced by a progressive surface wave are nominally two-dimensional with components (u, w) and $(\dot{u}, \dot{w})$, respectively. The u components coincide with the direction of wave advance while w and $\dot{w}$ occur in the vertical direction. Short-crested or multi-directional seas will produce additional components of velocity and acceleration. In order to apply Morison's equation to such a complex flow field some adaptations and simplifications are required. This section considers the common approximations and simplifications in order to assess their influence on the accuracy of predicted wave forces and to assess their effects on computed force coefficients.

The additional hydrodynamic complexities that are encountered in wave flows may be summarized as follows.

- The flow is not always perpendicular to the cylinder axis.
- The wake is not always swept back and forth over the cylinder.
- The flow is not always uniform along the span.
- The flow velocities and accelerations are not explicitly known.

The first two effects are largely determined by the eccentricity of the water particle orbits and by the orientation of the cylinder with respect to the orbits [12]. The variation of the flow along the span will introduce three-dimensional effects in a number of ways. Obviously, the instantaneous velocities and accelerations will have an axial variation which can alter the flow forces away from the distribution predicted using one-dimensional results. Less obvious is the three- dimensional effect arising from the wake which may be swept back over or near one segment of the cylinder after being generated at another segment under different flow conditions.

Three-dimensional effects have been observed to have a pronounced influence on the drag in steady bluff body flows [13, 14].

The flow velocities and accelerations are usually computed from a particular wave theory which has been matched to the wave shape. Since different wave theories will, in general, produce different pairs of force transfer coefficients for the same data, it is often suggested that the user be consistent in the selection of wave theory [1]. Many investigators have employed higher-order expansions, e.g. — Stokes 5th order, in wave force computations and report improved matching to the wave force [2]. In all likelihood these improvements are largely a result of the additional terms in the curve fitting function and bear little relation to any improvements in the hydrodynamic description as discussed in the following. In many instances the usual approach reduces to a selection of a wave theory that best matches the *observed wave surface profile* or, in other words, the velocity and acceleration fields are obtained by matching computed and observed *displacements* at the free surface. Since the velocity and acceleration are essentially derivatives of displacement it is clear that a good match to the surface displacements does not insure an equally good match to the interior kinematics of the flow. Stokes expansions are routinely invoked for describing the kinematics of finite-height waves, so that it is constructive to examine their use.

First, the dynamical surface boundary condition can be used to illustrate the problems of obtaining velocities from a matching of surface displacements. Let the surface elevation η be expanded in the regular perturbation series

$$\eta = \eta_o + \eta_1\epsilon^2 + \eta_3\epsilon^3 + 0(\epsilon^4) \tag{3.1}$$

where $\epsilon << 1$ is the wave slope. The velocities and accelerations can be similarly expanded but not to the same order of accuracy if the dynamical boundary condition given by

$$\frac{\partial\phi}{\partial t} + 1/2(u^2 + w^2) - g\eta = 0 \tag{3.2}$$

is to be uniformly satisfied. In particular, the quadratic terms in the velocity require that a remainder of order ϵ^n in the surface displacement will correspond approximately to a remainder of order $\epsilon^{n/2}$ in the velocity expansion. Hence, the use of such expansions will require a disproportionately large number of terms to significantly improve the representations of velocity and acceleration beyond their linear descriptions. In view of the ease of superposition of linear waves and the practical importance of directionality and short-crested seas, higher order expansions or theories hardly seem worthwhile except possibly in the extreme, single design wave approach. The use of Stokes-type expansions can also introduce other sources of error and uncertainty as described below.

The two problems of interest are the use of Morison's equation to predict wave forces and the use of Morison's equation to obtain the force coefficients C_M and C_D from a wave force record. To begin, let the velocity expansion be written symbolically as

$$u = \sum_{n=1}^{r} U_n \cos n\theta, \tag{3.3}$$

so that the acceleration is given by

$$\dot{u} = \frac{2\pi}{T} \sum_{n=1}^{r} U_n \sin n\theta, \tag{3.4}$$

where r represent the order of the expansion and $\theta = kx - wt$. This notation is adopted for convenience and it should be noted that the forms of the coefficients U_n depend on both n and r. To simplify the discussion, the usual Morison approach is taken for a horizontal cylinder in waves so that so the nondimensional force becomes

$$f_x(\theta) = C_D \sum_{n=1}^{r} \sum_{j=1}^{r} \frac{U_n U_1}{U_1^2} \cos n\theta |\cos j\theta| + \frac{\pi^2}{K} C_M \sum_{n=1}^{r} n \left[\frac{U_n}{U_1}\right] \sin n\theta \tag{3.5}$$

when the characteristic velocity U_m is equal to U_1, a constant. As expected, a large number of harmonics are rapidly introduced. For fixed values of the coefficients C_M and C_D the presence of these harmonics can be examined by looking at the first few contributions from Stokes second-order wave theory where

$$U_1 = \frac{\cosh k\ (d + z)}{\sinh kd} \tag{3.6a}$$

and

$$U_2 = \frac{3}{4}\left[\frac{\pi H}{L}\right]\frac{\cosh 2k\ (d + z)}{\sinh 4\ kd} \tag{3.6b}$$

with d being the water depth, k the wavenumber $\frac{2\pi}{L}$, H the waveheight, and z the depth of the cylinder below mean water level. The two additional drag terms are

$$\frac{U_2}{U_1}\left(|\cos 2\theta|\cos\theta + \cos 2\theta|\cos\theta|\right) \tag{3.7a}$$

and

$$2\left(\frac{U_2}{U_1}\right)^2(\cos 2\theta|\cos 2\theta|) \tag{3.7b}$$

while the additional inertia term is

$$2\left(\frac{U_2}{U_1}\right)\sin 2\theta \tag{3.7c}$$

one of which is plotted in Figure 4. The proliferation of harmonics is quite clear and their importance depends directly on the ratio U_2/U_1. For deep water waves of any realizable steepness this ratio is quite small. For a wide range of other wave conditions this ratio remains small enough that the use of Stokes expansions can be avoided.

It is perhaps more interesting to examine the complementary problem of obtaining C_M and C_D from the same wave force record using different order Stokes wave theories. The integral least-squares results, Eqs. 2.18 and 2.19, can be generalized to permit arbitrary (but orthogonal) velocities and accelerations as follows

$$C_D = \frac{\int_o^{2\pi} f_{meas}\, u|u|\, d\theta}{\int_o^{2\pi} (u|u|)^2\, d\theta} \tag{3.8}$$

$$C_M = \frac{\int_o^{2\pi} f_{meas}\, \dot{u}\, d\,\theta}{\int_o^{2\pi} \dot{u}^2\, d\theta}. \tag{3.9}$$

The expression for C_M is easier to deal with and an important point can be made using it alone. Upon substitution of $\dot{u}$ from Eq. 3.4 the expression for C_M becomes

$$C_M = \frac{k}{\pi^3} \frac{1}{\Sigma U_n^2 n^2} \cdot \int_0^{2\pi} f_m \, (\Sigma \, U_n \sin n\theta) \, d\theta \tag{3.10}$$

in analogy with earlier expressions. Next let the non-dimensional measured force be separated into its Fourier components as follows

$$f_{meas}(\theta) = \sum_{n=1}^{\infty} (a_n \sin n\theta + b_n \cos n\theta). \tag{3.11}$$

Upon substitution into Eq. 3.9 the result is

$$C_M = -\frac{2T}{\pi^2 \rho D^2 L \, \Sigma \, U_n^2} \, a_1 U_1 + a_2 U_2 + a_3 U_3 + \ldots \tag{3.12}$$

as one would expect. This result is however based on the assumption that the harmonics in the measured force are solely a result of the harmonics in the acceleration. If harmonics occur for some other reason then this approach cannot distinguish their origin and simply lumps the effect into the computed coefficient and by definition will give a good fit to the data. The problem once again is to attach any general significance to the coefficient so obtained. A natural question concerns the type of harmonic structure that can be expected for various flows.

Sarpkaya largely neglects the higher harmonics and thereby implies their smallness. On the other hand Keulegan & Carpenter devoted significant effort to categorizing the higher harmonics or, as they termed it, the residual force. The observed residual force was greatest in the neighborhood of $K = 15$ which is usually associated with asymmetric vortex-shedding. The peak residual force was as much as twenty percent of the peak force and had components at both cos 3θ and sin 3θ. It seems that these variations in the in-line force correspond to some of the largest changes in the transverse or lift force. Due to the orbital motion of the fluid, a measurement of the horizontal component of force $f_x(\theta)$ on a horizontal cylinder will at times contain a component of the lift force generated by the vertical component of velocity. Since

this usually oscillates at a multiple of the wave frequency, it will appear as a harmonic in the force record and in view of the above equation it can lead to an improper computation of the coefficients. Thus, higher-order wave theories must be applied with some care in order to obtain consistent results and in order not to mask some of the physical differences between various situations. By the same token it may be possible to identify the various physical processes by carefully analyzing the changes in harmonic structure. It is interesting to note that Chakrabarti's experiments with inclined cylinders in waves produced the largest residual force variations at *twice* the wave frequency [10,11] as compared to 3θ for Keulegan & Carpenter. As a final comment, the sensitivity to harmonics of single-point methods for obtaining C_M and C_D is evident in the above expressions.

There are many possible wave-cylinder configurations, but two particular cases are studied here to isolate, as far as possible, two different *physical* situations. The first configuration is a horizontal cylinder whose axis is parallel to the wave crests. As in a simple oscillating flow, the velocities and accelerations are always normal to the cylinder axis and it is possible to select a diameter that is small compared to the scale of the vertical gradients of velocity and acceleration. Under these conditions one would expect some correspondence between a wave flow and the simple oscillating flow. The principal differences are due to the eccentricities of the water particle orbits under waves, such that the wake is not always swept back over the cylinder. The vertical cylinder case admits the axial variation of velocity and generally the velocities and accelerations are no longer normal to the cylinder axis. On the other hand, the wake is swept back and forth over the vertical cylinder as it is in the one-dimensional case.

3.1 *Horizontal Cylinder* — Even with the available simplifications it is not obvious what form Morison's equation should take for wave flows about a horizontal cylinder. This is due to

the second components of velocity and acceleration. It has become customary to write Morison's equation for each component of force using the corresponding components of velocity and acceleration to obtain

$$f_x(\theta) = C_D \frac{u|u|}{U_m^2} + \frac{\pi^2}{K} C_M \frac{\dot{u}}{2\pi U_m/T} \tag{3.13}$$

and

$$f_z(\theta) = C_D \frac{w|w|}{U_m^2} + \frac{\pi^2}{K} C_M \frac{\dot{w}}{2\pi U_m/T} \tag{3.14}$$

where U_m is as yet an unspecified characteristic velocity and the subscripts refer to the component directions. It is also possible to write Morison's equation using vector quantities and then to take the components of the resultant vector force so that

$$f_x(\theta) = C_D \frac{qu}{Q^2} + \frac{\pi^2}{K} C_M \frac{\dot{u}T}{2\pi Q} \tag{3.15}$$

and

$$f_z(\theta) = C_D \frac{qw}{Q^2} + \frac{\pi^2}{K} C_M \frac{\dot{w}T}{2\pi Q}, \tag{3.16}$$

where

$$\vec{q} = u\hat{i} + w\hat{k} \tag{3.17a}$$

and

$$q = \sqrt{u^2 + w^2}, \tag{3.17b}$$

$$Q = \sqrt{U^2 + W^2} \tag{3.17c}$$

The second pair of equations for the force components are seldom employed even though they appear somewhat more rigorous. It must be emphasized that both approaches reduce to the one-dimensional case *and* both give a good fit to the data *but* for different values of the coefficients C_D and C_M.[1] This is the crux of the problem because a common objective (and one objective of this investigation) is to determine what form of the Morison equation is valid for wave flows *and* whether or not the coefficients obtained from a one-dimensional experiment

[1]The linearity of the inertia term often results in no difference between the two approaches.

are useful in a two-dimensional wave flow. Clearly, the choice between Eqs. 3.1 and 3.2 or Eqs. 3.3 and 3.4 will have to be made with the aid of experimental results and a careful comparison with one-dimensional results.

Although the vector approach appears to yield the more complex expressions, the particular case of deepwater waves produces a simpler expression for the drag force and no difference at all between the inertia force terms. For a horizontal cylinder at a depth $z = -d_c$ we have from linear wave theory

$$u(t) = \frac{\pi H}{T} e^{-kd_c} \cos\theta, \quad \dot{u}(t) = \frac{2\pi^2 H}{T^2} e^{-kd_c} \sin\theta \tag{3.18}$$

and

$$w(t) = \frac{\pi H}{T} e^{-kd_c} \sin\theta, \quad \dot{w}(t) = \frac{2\pi^2 H}{T^2} e^{-kd_c} \cos\theta$$

where $\theta = kx - \omega t$. By defining $U_m = \frac{\pi H}{T} e^{-kd_c}$ the drag terms in Eqs. 3.13 and 3.14 become

$$f_{Dx}(\theta) = C_D \cos\theta|\cos\theta| \tag{3.19}$$

and

$$f_{Dz}(\theta) = C_D \sin\theta|\sin\theta|. \tag{3.20}$$

The drag terms in Eqs. 3.3 and 3.4 take the alternate forms

$$f_{Dx}(\theta) = C_D \cos\theta \tag{3.21}$$

and

$$f_{Dz}(\theta) = C_D \sin\theta. \tag{3.22}$$

The difference between the two pairs of expressions is significant in that both give the same peak drag force but for the remainder of the cycle the second pair predict larger drag forces than the first. For example, at $\theta = \pi/4$ the second approach gives a drag 40 percent larger than the usual approach for equal peak values. In a situation where the drag and inertia forces are comparable in magnitude this difference means about a 20 percent change in the

predicted peak wave force. Therefore, the proper selection of approach, i.e. component versus vector, has important consequences other than the matter of specifying C_M and C_D. An experiment that measures both components of force on a horizontal cylinder under waves can be expected to resolve this question, but owing to vortex-induced side force this will not be as straightforward as it might appear [10, 11].

3.2 *Vertical Cylinders* — As in a planar flow the vortex wake of a vertical cylinder in waves is swept back and forth over the cylinder. However, the flow usually varies in direction with time and varies in magnitude along the span. The usual approach is to write Morison's equation in a differential form, take the components of velocity and acceleration normal to the cylinder, and then integrate over the length of the cylinder to get the total in-line force. The key assumption is that C_M and C_D can be taken as uniform along the span to get

$$f = C_D \cos\theta|\cos\theta| \int_{-z_b}^{\eta} a^2 dz - C_M \pi^2/K \sin\theta \int_{-z_b}^{\eta} a dz \tag{3.23}$$

where

$$a = \cosh kz + \tanh kd \sinh kz \tag{3.24}$$

for a cylinder extending from a depth $z = -z_b$ to the instantaneous free surface η. It is also customary to evaluate the coefficients at the still water level, which is to say that the characteristic velocity U is the horizontal velocity at $z = 0$. The obvious difficulty with this approach is its inability to account for different vertical distributions which may have the same characteristic velocity U. For example, two cylinder-wave combinations, one a deepwater wave and one a shallow water wave, can be selected to give the same values of K and β at $z = 0$, but the vertical distributions of C_M and C_D can be quite different. The discrepancy is potentially greater when the differences in orbital motions are considered as well. A simple correction can be obtained by assuming a linear distribution of C_M, fitting this to the data and then comparing the linear distribution to a distribution constructed from the planar flow results. Since the total inertia component of force is the same regardless of the choice of description we have

$$C_M \int_{-z_b}^{\eta} a \sin\theta \, dz = \int_{-z_b}^{\eta} (C_{M_1} + C_{M_2} z) \, a \sin\theta \, dz \tag{3.25}$$

where

C_M = the best fit constant coefficient.

C_{M_1} = the $z = o$ value of a linear distribution, and

C_{M_2} = the slope of the linear distribution.

This expression can be used to estimate the slope of a "best fit" linear distribution by setting C_M equal to the coefficient obtained using Eqs. 3.1 and 3.2 and setting C_{M_1} equal to the corresponding planar flow value. For simplicity and in view of the approximate nature of this approach the upper limit of integration is taken as $z = o$ to get

$$C_{M_2} = (C_M - C_{M_1}) \frac{\int_{-z_b}^{o} a \, dz}{\int_{-z_b}^{o} za \, dz} \tag{3.26}$$

where the integrals are easily evaluated for each wave condition. A similar analysis for the drag term yields

$$C_{D_2} = (C_D - C_{D_1}) \frac{\int_{-z_b}^{o} a^2 dz}{\int_{-z_b}^{o} za^2 dz} \tag{3.27}$$

With these expressions it will be possible to examine, in a rudimentary way, the effects of flow gradients along the cylinder axis upon the individual drag and inertia components of the wave force.

4.0 PRESENTATION AND DISCUSSION OF EXPERIMENTAL RESULTS

The present results were obtained for relatively low Reynolds numbers, $Re \approx 10^3 - 4 \times 10^3$, and for values of the frequency parameter in the range β = 300-700. The depths of the horizontal cylinders varied between three and twelve cylinder diameters below still water level while the vertical cylinders were positioned to pass through the free surface at all times and terminate some distance (approx. 12 cyl. dia.) from the bottom of the tank.

4.1 *Horizontal cylinders.* Despite the common use of horizontal or near horizontal structural members in many offshore platforms, little work has been done regarding horizontal cylinders under waves. From a hydrodynamic viewpoint the wave flow about a horizontal cylinder is interesting because of certain similarities to the planar flow case. Namely, the flow is uniform over the span and is always perpendicular to the cylinder axis. The significant differences are due to the orbital motions under waves such that the wake is not always swept back and forth over the cylinder.

A recent paper by Maull & Norman [8] considered the horizontal cylinder under waves and represented the measured force by RMS coefficients defined as

$$C_F = \frac{(\text{Force}_x)_{rms}}{1/2\rho\ DL(U_{rms})^2} \tag{4.1}$$

for the force component in-line with the wave direction and as

$$C_L = \frac{(\text{Force}_z)_{rms}}{1/2\rho\ DL(W_{rms})^2} \tag{4.2}$$

for the component transverse to the wave direction. C_L is often referred to as a lift coefficient although this is potentially confusing because the transverse force in this case is also of the Morison-type. The characteristic velocities, U and W, are computed for the centerline depth of the cylinder.

Comparisons between the present results and those of Maull & Norman are presented in Figures 5 and 6. The coefficients are based on the RMS force components at the wave frequency. The comparisons can only be qualitative since the ratio of maximum vertical velocity W to maximum horizontal velocity U in the present experiments ranges from $W/U = 0.9$ to $W/U = 1.09$ while Maull & Norman's data were obtained for $W/U = 0.81$-0.84. Also, their velocities and accelerations were computed from Stokes second order theory whereas the present values were obtained from the linear theory. Maull & Norman do not give a range of β

values although the experimental description suggests that they should be close to the present values of $\beta = 450$ and $\beta = 630$. In spite of these differences the results of the two sets of experiments agree quite well. Also included in the figures are Maull & Norman's representations of the predicted RMS coefficients based on Sarpkaya's planar flow results. A substantial overprediction is observed although it must be noted that as W/U decreased Maull & Norman found that the RMS wave forces tended toward the one-dimensional results as might be expected.

The total in-line and transverse RMS coefficients for the present results are compared in Figure 7 to each other and to the planar flow results of Sarpkaya [5] and of Bearman, Graham & Singh [6]. The discrepancies between the two sets of one-dimensional results are unexplained but again either set will significantly over-predict the RMS wave force. It should also be noted that the RMS transverse or lift force is consistently less than the RMS in-line force for equivalent values of the Keulegan-Carpenter number.

The individual coefficients C_M and C_D can be determined once a suitable form of Morison's equation is adopted. The choices were described in Section 3.1 and amounted to either a scalar application of Morison's equation to the components of velocity and acceleration or a vector approach using the vectors of velocity and acceleration. The best fit of each method to a typical measured force record is presented in Figure 8 where it is evident that the vector approach is indeed more appropriate and suggests the use of Eqs. 3.3 and 3.4 for horizontal cylinder. In every case Eqs. 3.1 and 3.2 produce drag coefficients that are smaller (approx. 5-10%) than the drag coefficients obtained from Eqs. 3.3 and 3.4. The inertia coefficient is, of course, the same in each case. Another significant feature of the vector approach is the linearity of the resulting force components in deep water which will permit stochastic analysis of horizontal members without artificial linearization.

The least-squares, best fit inertia coefficients are presented in Figure 9 along with the one-dimensional results of Sarpkaya and of Bearman et al. As might be anticipated from the RMS coefficients, the wave-induced intertia forces are less than either set of planar flow results but appear to follow the same trend of decreasing C_M with increasing K. On the other hand the results for the drag coefficient exhibited a marked departure from the one-dimensional results as shown in Figure 10. Not only are the drag coefficients less than their planar flow analogues but they also do not contain the "hump" which is characteristic of C_D in this range of K. There is a suggestion that the present results might eventually merge with the planar flow results of Bearman et al. at larger values of K and this ought to be investigated further.

The difference in behavior between the wave drag coefficients and the planar flow drag coefficients must be explained on the basis of the orbital motions of the fluid. Physically, this is satisfying because the present range of Keulegan-Carpenter number corresponds to a relatively small number of vortices being shed during a flow cycle. If these few vortices are rectilinearly swept back over the cylinder then their influence on the nascent vortices, thence the force, is likely to be much larger or at least much different than a few vortices which are swept away during the orbital motion under waves. In a sense, the drag on a horizontal cylinder under waves is more akin to the steady flow drag than to the 1-D unsteady drag. Thus, the "hump" behavior will not occur for horizontal cylinders and the drag coefficient appears to monotonically approach the steady-state drag coefficient as the Keulegan-Carpenter number increases. This limit has been demonstrated by Bearman et al. for a variety of body shapes in planar flows at large K [6].

4.2 *Vertical cylinders*— The present results are listed together with corresponding one-dimensional data in Table 1. The one-dimensional values were obtained from Sarpkaya [5] because his data are quite extensive. Even so, it was often necessary to interpolate and, in

Table 1 — Vertical Cylinder Results

$K)_{z=0}$	$\beta)_{z=0}$	Total Meas. RMS Force	Total Pred. RMS Force	RMS Inertia Force Ratio	RMS Drag Force Ratio	C_M	C_D	W/U	$\left.\frac{du}{dz}\right\|_{z=0}$	C_L
5.8	701	1.16	2.18	0.58	0.05	0.76	0.11	0.94-1.0	0.81	0.08
8.2	454	1.44	2.58	0.55	0.18	0.66	0.36	0.62-0.98	0.31	0.16
11.3	573	0.74	1.36	1.01	0.12	0.65	0.26	0.81-1.0	0.87	0.06
11.4	619	0.72	1.48	1.01	0.14	0.72	0.30	0.87-1.0	1.11	0.06
12.7	395	1.12	2.56	0.92	0.17	0.65	0.29	0.52-0.95	0.31	0.17
13.6	526	0.70	1.80	0.86	0.16	0.58	0.36	0.74-1.0	0.81	0.08
13.7	451	1.06	2.42	0.93	0.26	0.62	0.63	0.62-0.98	0.51	0.18
18.0	312	1.16	3.26	0.90	0.22	0.68	0.43	0.41-0.87	0.21	0.35

some instances, to extrapolate the one-dimensional data so that the comparisons should only be viewed as qualitative. Had the one-dimensional results of Bearman et al. [6] been used, the comparisons between wave results and planar flow data would be more favorable but the same general discrepancies would occur. The total wave force, as measured by the RMS value, is again over-predicted by the planar flow results but it is not obvious whether this is due to inappropriate coefficients of drag and inertia due to the assumption of uniform coefficients over the span or due to the combination. To begin to resolve this question the individual RMS components of drag and inertia were compared to their predicted values and the ratios are listed in Table 1. Evidently, the overprediction is principally in the drag contribution since the ratio of measured and predicted RMS inertia forces is close to one. In fact, the values are close enough to suggest that a correction for the distribution of C_M may be able to account for the discrepancy. A simple estimate of the correction can be obtained by assuming a linear distribution of C_M, fitting this to the data and then comparing the linear distribution to a distribution constructed from the planar flow results as discussed in Section 3.2. Plots which are typical of the results that can be obtained are presented in Figure 11. Since the inertia force decays essentially exponentially with depth in the present experiments it is clear that the actual C_M distribution is well represented by a distribution constructed from one-dimensional flow results.

Alternatively, a uniform value can be assumed and the error in doing so can be estimated from one-dimensional results using Eq. 3.26. A plot of this estimate of the error is given in Figure 12.

A similar analysis of the drag component is far less fruitful because of the large disparities between the observed and the predicted drag. The disparity in each case can be attributed to either the variation in the velocity along the span or to the variation in the flow direction during the cycle or to both of these. During the present experiments the slopes of the velocity variation and the eccentricities of the water particle orbits varied from test to test. Unfortunately they often varied together and so it is not possible to separate the two effects. The eccentricities W/U and velocity variations, characterized by the slope at $z = 0$, are listed in Table 1. The apparent trend is that as the velocity variation decreases and/or the orbits flatten the drag tends toward the one-dimensional result. With further study, or possibly further analysis of existing wave force data, this approach could provide a basis for modifying one-dimensional results for use in wave force prediction. It would also be possible to establish error bounds for the assumption of a constant C_D.

The final entry in Table 1 is the measured RMS lift coefficient, which in this case is purely a vortex effect and is not described by Morison's equation. In the same sense that the velocity variation and orbit eccentricity influence the drag, one intuitively expects that the vortex-induced lift will be similarly influenced and indeed this appears to be the case. An important event which was observed during the experiments but masked by the RMS coefficient of lift was a significant peak in the lift that occurred near the crest of the wave. The peak resultant force in those cases was much larger than expected from any combination based on the RMS values of the in-line and the lift force. This has been discussed elsewhere [5, 7] and is only mentioned here as a reminder.

5.0 SUMMARY AND CONCLUSIONS

The results of the present investigaton have shown that the resolution of a Morison-type approach to wave force prediction can be improved if consistent methods of computation are employed along with some accounting for the major differences between wave-induced vortex flows.

In the case of a horizontal cylinder in waves the horizontal and vertical components of the wave force must be obtained from a modified form of Morison's original equation whereby each component is derived from an equation written for the instantaneous total force. The modified equations are linear and are therefore readily employed in stochastic analyses. The force transfer coefficients C_M and C_D for the horizontal cylinder cannot be obtained from one-dimensional planar flow results except possibly at large Keulegan-Carpenter numbers. The planar flow coefficients can overpredict the actual wave force on a horizontal cylinder in waves by as much as 100 percent. The present results along with some simple physical arguments suggest that the drag coefficient on the horizontal cylinder rapidly approaches the steady flow value for increasing Keulegan-Carpenter number and does not exhibit the "hump" behavior which is characteristic of unsteady planar flows.

The wave forces on vertical cylinders were decomposed into inertial and drag contributions for which vertical distributions were estimated. It was shown that the usual assumption of uniform C_M and C_D can lead to significant errors but that a distribution of C_M based on one-dimensional results adequately accounts for the wave-induced inertia force. On the other hand, the one-dimensional flow drag coefficients greatly overpredict the wave-induced drag and the amount is attributed to the "steepness" of the velocity gradient along the span and to the eccentricity of the water particle orbits.

The implications of the present findings for the wave-induced forces on inclined cylinders and for the forces on cylinders in short-crested seas are straightforward. When the various hydrodynamic complexities associated with wave flows were isolated as much as possible, it was found that a reduction in force occurred as compared to one-dimensional results. Thus it may be expected that situations where all or most complexities occur together, such as inclined cylinders or short-crested seas, a further reduction in wave force is likely. Predictions based on results from other configurations, particularly one-dimensional flows, will be very conservative.

ACKNOWLEDGMENTS

The authors acknowledge the support of the Naval Research Laboratory for the experiments reported in this paper.

6.0 REFERENCES

1. Hogben, N., Miller, B.L., Searle, J.W. and Ward, G., "Estimation of Fluid Loading on Offshore Structures," Proc. Inst. Civil Engineers, Vol. 63, Part 2 (1977) pp. 515-562.

2. Miller, B.L. and Matten, R. B., "A Technique for the Analysis of Wave Loading Data Obtained from Model Tests," NPL Report Mar Sci R136 (June 1976).

3. Morison, J.R., O'Brien, M.P., Johnson, J.W., and Schaaf, S.A., "The Force Exerted by Surface Waves on Piles," Trans. American Inst. Mining and Metallurgical Engineers, Vol. 189 (1950) pp. 149-154.

4. Sarpkaya, T., "Forces on Cylinders and Spheres in a Sinusoidally Oscillating Fluid," Trans. ASME, Journ. Applied Mechanics, Vol. 42, No. 1 (1975) pp. 32-37.

5. Sarpkaya, T. "In-Line and Transverse Forces on Cylinders in Oscillatory Flow at High Reynolds Numbers," Journ. Ship. Res., Vol. 21, No. 4 (1977) pp. 200-216.

6. Bearman, P.W., Graham, J.M.R., and Singh, S., "Forces on Cylinders in Harmonically Oscillating Flow," Proc. WIFOC '78 Symp., Briston, U.K. (1978).

7. Bearman, P.W., Graham, J.M.R., "Hydrodynamic Forces on Cylindrical Bodies in Oscillatory Flow," Proc. 2nd Int. Conf. on Behavior of Off-Shore Structures, (BOSS paper 24), London, U.K. (1979) pp. 309-322.

8. Maull, D.J. and Norman, S.G., "A Horizontal Circular Cylinder under Waves," Proc. WIFOC '78 Symposium, Bristol, U.K. (1978).

9. Keulegan, G.H. and Carpenter, L.H., "Forces on Cylinders and Plates in an Oscillating Fluid," J. of Research of Nat. Bureau of Standards, *Vol. 60, No. 5* (1958).

10. Bidde, D.D., "Laboratory Study of Lift Forces on Circular Piles," Journ. of the Waterways, Harbors and Coastal Engineering Div., ASCE, Vol. 97, No. WW4, (1971) pp. 595-614.

11. Isaacson, M. de St. Q. and Maull, D.J., "Transverse Forces on Vertical Cylinders in Waves," Journ. of the Waterways, Harbors and Coastal Engineering Div. ASCE, Vol. 102, No. WW1, (1976) pp. 49-60.

12. Chakrabarti, S.K., Tam, W.A. and Wolbert, A.L., "Total Forces on a Submerged Randomly Oriented Tube Due to Waves," OTC paper 2495 (1976) pp. 723-739.

13. Pearcey, H.H., "Some Observations on Fundamental Features of Wave-induced Viscous Flows Past Cylinders," Proc. WIFOC '78 Symp., Bristol, U.K. (1978).

14. Graham, J.M.R., "The Effect of End-Plates on the Two-dimensionality of a Vortex Wake," Aero. Quarterly, Vol. 20, (1969) pp. 237-247.

15. Ramberg, S.E., "The Influence of Yaw Angle upon the Vortex Wakes of Stationary and Vibrating Cylinders," NRL Memorandum Report 3822 (1978).

16. Holmes, P. and Chaplin, J.R., "Wave Loads on Horizontal Cylinders," Proc. 16th Int. Conf. on Coastal Eng., Hamburg, Germany (1978).

17. Wolberg, J.R., *Prediction Analysis*, Van Nostrand Co. Inc., Princton, N.J. (1967).

18. Griffin, O.M. and Wright, J.W., "A New Wave-Wind Channel For Fluid Dynamics Research at the Naval Research Laboratory," NRL Memorandum Report 3352 (1976).

APPENDIX A
The Least-Squares Error Method

There are a number of methods that can be used to determine the coefficients C_M and C_D for a particular form of Morison's equation and a certain set of data. The most common and widely accepted methods involve Fourier analysis or curve-fitting or both. A complete description of Fourier analysis can be found in most standard math texts but descriptions of curvefitting methods are usually restricted to the simplest case(s). For this reason a brief review of the general least-squares curvefit is given here and the reader is directed to a book by Wolberg for a full description [17].

The first step in any curvefit is to assume that a "true" relationship exists in the form

$$\eta = f(\xi_1, \xi_2, \xi_3, \ldots \xi_n, \alpha_1, \alpha_2, \alpha_3 \ldots \alpha_m) \tag{A1}$$

where

η is the dependent variable,
ξ_i are the n *true independent variables,*
α_i are the m *true coefficients, and*
$f(\ )$ is the *true relationship.*

The objective is to construct the best representation of this relationship using measured values of the independent variables X_{ki} and measured values of the dependent variable Y_k. The constructed equation is written as follows

$$y_k = f(x_{k1}, x_{k2}, x_{k3}, \ldots x_{ki}, a_1, a_2, a_3, \ldots a_m) \tag{A2}$$

y_k is the k^{th} computed value of the dependent variable,
x_{ki} is the k^{th} computed value of the i^{th} independent variable, and
a_m are the computed coefficients.

The "best constructed equation" is defined as the equation whose values for the coefficients a_m

satisfy some minimum error criterion with a particular set of observed values Y_k and X_{kl}. It is customary to minimize the differences between the observed values and the calculated values in the least square sense. To do this we first must define the residuals,

$$\left.\begin{aligned} R_{yk} &\equiv Y_k - y_k \\ R_{xkl} &\equiv X_{kl} - x_{kl} \end{aligned}\right\} = \text{observed value - calculated value} \tag{A3}$$

and the weights,

$$\left.\begin{aligned} w_{y_k} &\equiv 1/\sigma^2_{y_k} \\ w_{x_{kl}} &\equiv 1/\sigma^2_{x_{kl}} \end{aligned}\right\} = (\text{standard deviation})^{-1}. \tag{A4}$$

The latter statistical weighting is adopted so that the residuals can be measured in units of standard deviation or, in other words, units of equal uncertainty. The computed values of a_m are sought which minimize the sum S of the squares of the weighted residuals

$$S = \sum_{k=1}^{p} \left\{ w_{y_k} R^2_{y_k} + \sum_{l=1}^{n} w_{x_{kl}} R^2_{x_{kl}} \right\}. \tag{A5}$$

The minimization of S is the general least squares curvefit. The solution procedure depends greatly on the form of the "true" relationship f and ultimately the form of S.

A few points are worth noting. First, the least squares curvefit does not determine if the assumed relationship is true or even if it is a good representation. The "goodness" of the assumed function must be judged by some other means such as its ability to match all or certain of the observed values of the dependent variable or perhaps its ability to produce certain values of the coefficients. The question of "goodness" becomes the question of the validity of Morison's equation for describing wave forces. In the case of wave forces, the judgement of "goodness" of Morison's equation can be made very difficult by the fact that the wave force is inherently periodic and the equation itself can be viewed as the first few terms of a Fourier expansion. Thus, a reasonably good fit can *always* be obtained quite apart from any *physical considerations* of the flow.

The second comment concerns the contribution of the independent variable residuals to the sum of the weighted, squared residuals. In most experiments the uncertainties in the independent variables are much smaller than the uncertainty in the dependent variable, i.e. $w_{x_{ik}} << w_{y_k}$, so that the sum S reduces to

$$S = \sum_{k=1}^{p} w_{y_k} R_{y_k}^2 \tag{A6}$$

and if w_{y_k} = constant $\equiv w$ then

$$S = w \sum_{k=1}^{p} (Y_{\text{observed}} - Y_{\text{calc}})^2 \equiv w\, E \tag{A7}$$

Now if the parameters a_m appear linearly in the assumed function, f, then the least square solution is obtained from the equations resulting from

$$\frac{\partial E}{\partial a_m} = 0. \tag{A8}$$

This is the commonest least-square solution and the one presented in most texts. The point to be made here is that this simple curvefit is often applied to the wave force problem without regard to the implications. Morison's equation relates the wave forces to the wave-induced velocities and accelerations but these quantities are rarely measured. Instead the velocities and accelerations are computed from a wave theory and the observed surface profile. This can be viewed as the assumption of another "true" relationship or as the introduction of significant residuals in the independent variables. In the first instance the "goodness" of Morison's equation cannot be separated from the "goodness" of the wave theory. In the second instance the simple curvefit procedure no longer applies and the general form of S must be employed with the introduction of more parameters. The general approach will not yield new or even very different answers but it would provide a rigorous basis for assessing the errors and ultimately the degree of confidence in the results obtained.

The final comment concerns the use of an integral representation of the error function to be minimized. These expressions are generally of the form

$$E = \int_o^T W(t)\ (Y_{obs} - Y_{calc})^2 dt = \int_o^T W(t) R^2(t)\ dt \tag{A9}$$

and the least-square solution is again found by

$$\frac{\partial E}{\partial a_m} = 0 \tag{A10}$$

provided that E is linear in the unknown coefficients a_m. Obviously, this error criterion is the limiting case of the earlier discrete summation and is strictly defined only when $W(t)$ and $R(t)$ are continuous or piece-wise continuous functions. If one wishes to apply the integral error criterion to a discrete function then some care must be taken in evaluating the integral so that arbitrary statistical weightings are not introduced. For example, the integral may be evaluated by simple rectangular segments to obtain

$$E = \int_o^T w(t)\ R_i^2(t)\ dt \approx \sum_{i=1}^{p-1} W(t_i)\ R^2(t_i)\ \Delta t_i \tag{A11}$$

or by Simpsons rule to obtain

$$E \approx \frac{1}{3}\Delta t[W(t_1)\ R_1^2 + W(t_p)\ R_p^2] + \frac{4}{3}\Delta t \sum_{i=2}^{p-1} w(t_{2i}) \cdot R_{2i}^2 + \frac{2}{3}\Delta t \sum_{i=2}^{p-1} w(t_{2i-1})\ R_{2i-1}^2 \tag{A12}$$

which on comparison with the usual discrete form

$$= \sum_{i=1}^{p} w_{F_i} R_i^2 \tag{A13}$$

shows that the choice of method to evaluate the integral can produce very different statistical weightings which will lead to different least-squares solutions. The integral operator has the advantage of simplifying many calculations so it is of interest to know the conditions that lead to the proper discrete, least-squares solution. Comparing Eqs. A11 and A13 and keeping in mind that the solution will be given by Eq. A10, it is clear that uniform statistical weighting and uniform sampling intervals Δt will permit the interchangable use of integral and discrete expressions *provided* that the integral is evaluated simply (i.e. — by means of a rectangular or a trapezoidal rule).

APPENDIX B
Experimental Systems and Methods

The experiments were performed in a 100 ft (30.5m) long, 4 ft (1.2m) wide, and 6 ft (1.8m) high wave tank at the Naval Research Laboratory [18] (see Figure B1). The tank was filled to a 3-1/2 ft (1.1m) depth during the tests. A one inch (2.54cm) diameter cylinder, 3 ft (0.9m) long, was placed in a U-shaped frame with two-component force gages at each end. The frame could be positioned so that the cylinder was either vertical or horizontal. In the horizontal configuration the bulk of the support frame was above water and the entire assembly was raised or lowered to achieve the desired cylinder depth. For the vertical cylinder tests the U-shaped frame was fastened to a vertical strut near one side of the channel so that the measurement cylinder was centered in the flume. The gap between the measurement cylinder and the nearest vertical support member was greater than 12 cylinder diameters. End effects [14] were not examined in this study but will be the subject of subsequent work on horizontal cylinders in waves.

The force gages were assembled as square-section cantilever beams with full-bridge straingage circuits arranged to sense orthogonal components of only the force applied to normal to the beam's end. The cylinder, force gage, and U-frame assembly was statically calibrated by applying known deadweights at various positions and directions along the cylinder. The linearity of the output as well as the proper partitioning of the load between the sensors at each end is indicated in Figure B2. From these tests the equivalent load for a precision shunt resistor across one arm of the bridge was also determined so that the resistor could be switched into the circuit for later check calibrations. The signals from the four DC bridge circuits were amplified

and filtered (Preston DX-1 amplifiers) before plotting on a strip chart recorder. The dynamic response of the force measurement and recording system was checked by pendulum oscillations of the deadweights. The phase shifts between the applied signals and the recorded results were undetectable (less than 0.01T for $0 \leqslant 1/T \leqslant 2$hz and less than 0.05T for $2 < 1/T \leqslant 10$hz).

After recording the data on strip charts several consecutive cycles were digitized, by hand, and stored on tape for processing with a desktop computer (Tektronix 4051).

The period and height of the incident wave were set by the motions of a mechanical, bulkhead-type wave generator located at one end of the channel [18]. For the present range of conditions, 98 percent or more of the generated wave energy was absorbed by a porous, sloping beach at the other end of the channel. The instantaneous water elevation at the cylinder was recorded and digitized in the same manner as the forces with a capacitance-type wave gage as the sensor. The measurement system was calibrated before each run and checked after each run. The accuracy of all measurements is believed to be better than ± 2 percent.

The force transfer coefficients were obtained from the digitized wave force record by the least-squares criterion,

$$S = \sum_{i=1}^{N} (f_{meas.} - f_{calc.})^2 \tag{B1}$$

subject to

$$\frac{\partial S}{\partial C_m} = \frac{\partial S}{\partial C_D} = 0 \tag{B2}$$

where N is the number of data points in the cycle which varied from 20 to 35. The wave-induced velocities and accelerations were computed using linear wave theory.

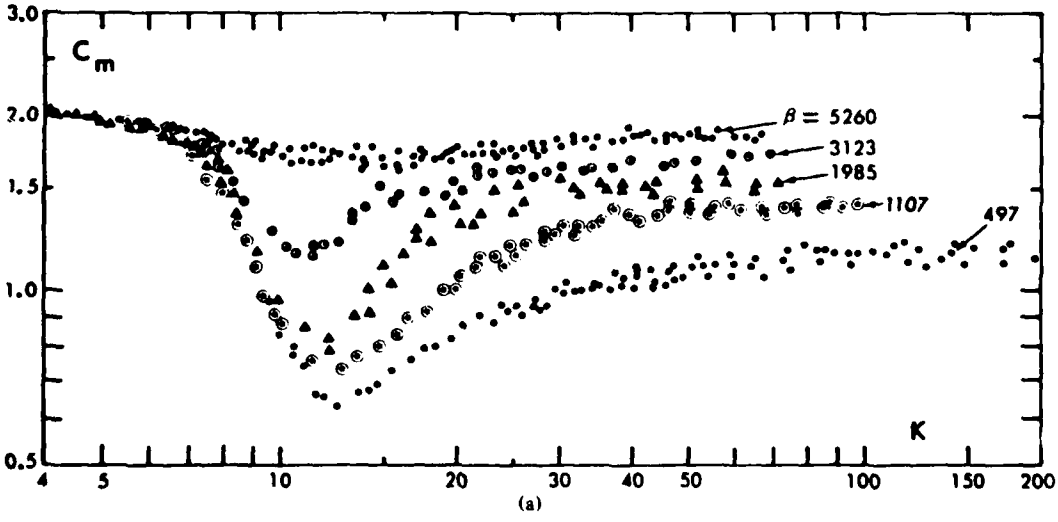

(a)

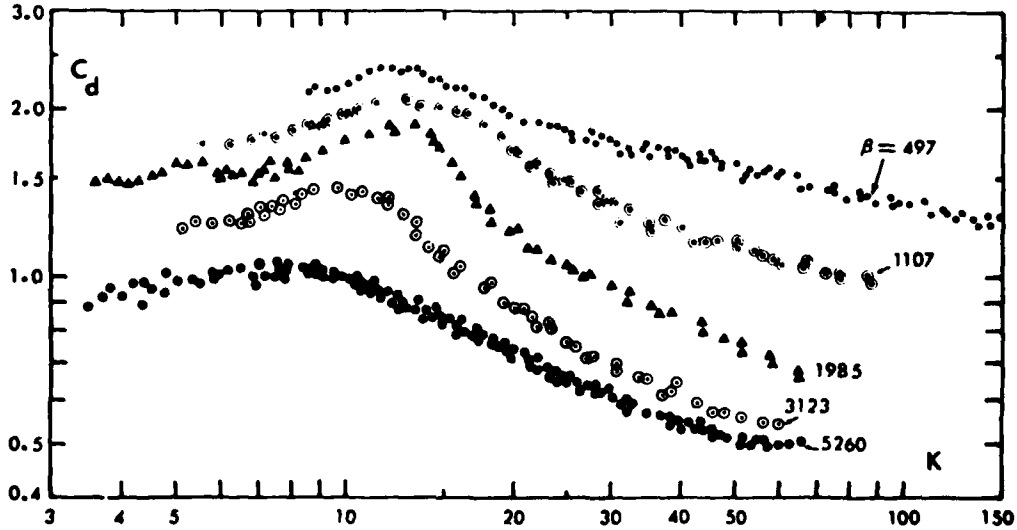

(b)

Figure 1 — Force transfer coefficients for one-dimensional oscillatory flow past circular cylinders from Sarpkaya [5]; a) inertia coefficients, b) drag coefficients.

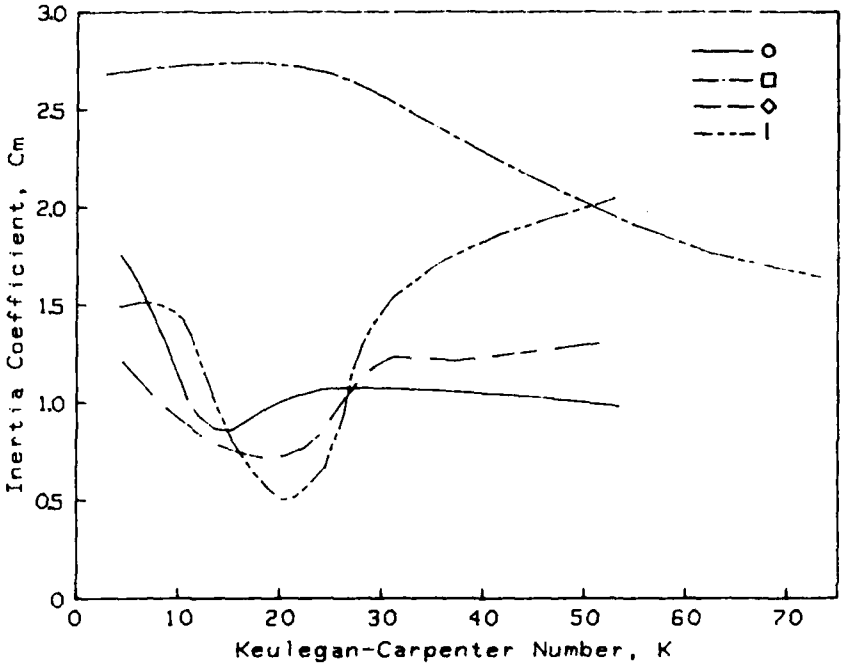

(a)

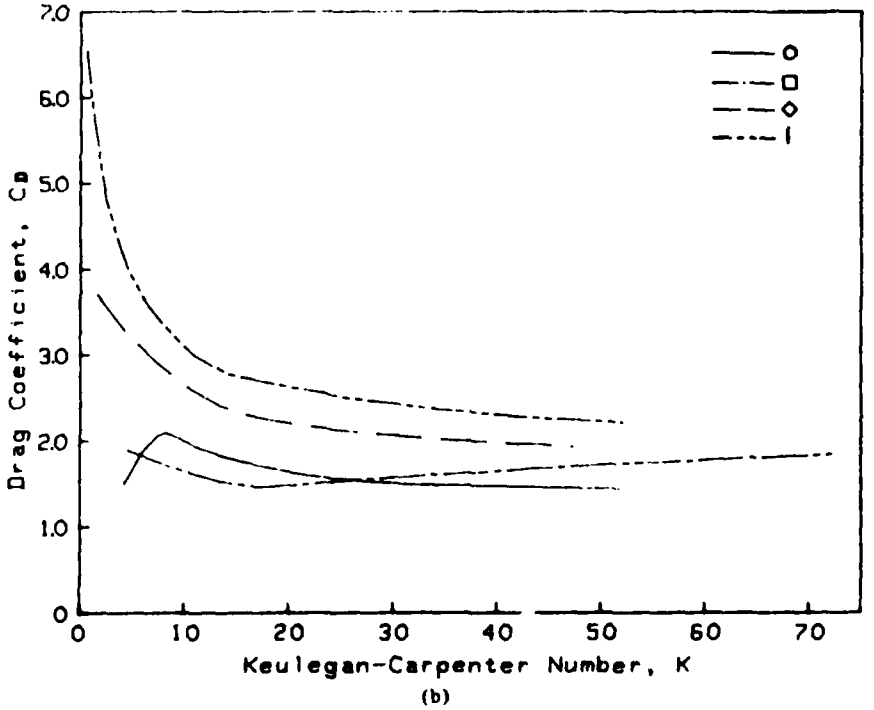

(b)

Figure 2 — Force transfer coefficients for one-dimensional oscillatory flow past variously shaped cylinders from Bearman et al. [6, 7]: a) inertia coefficients, b) drag coefficients.

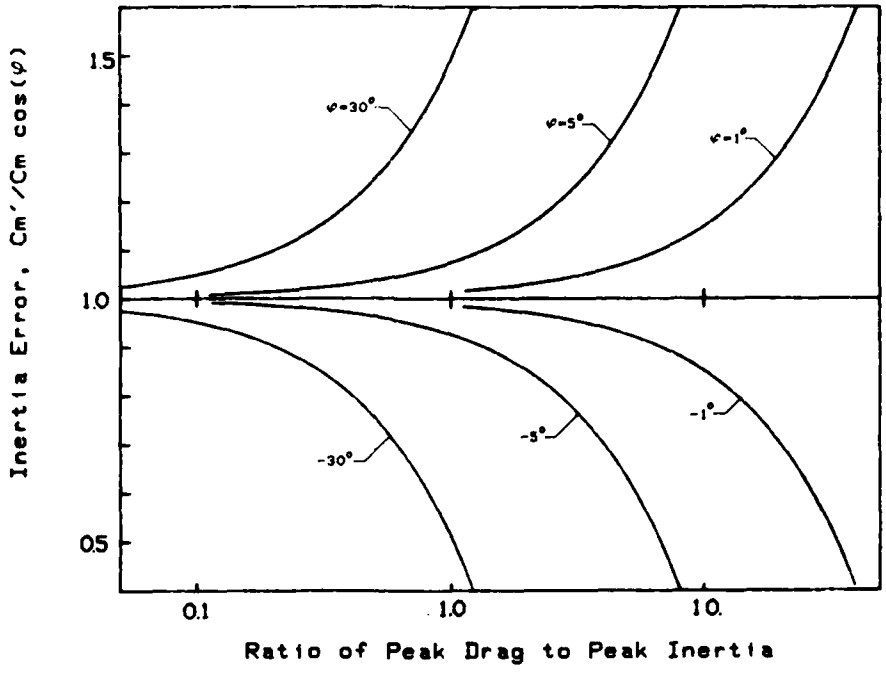

(a)

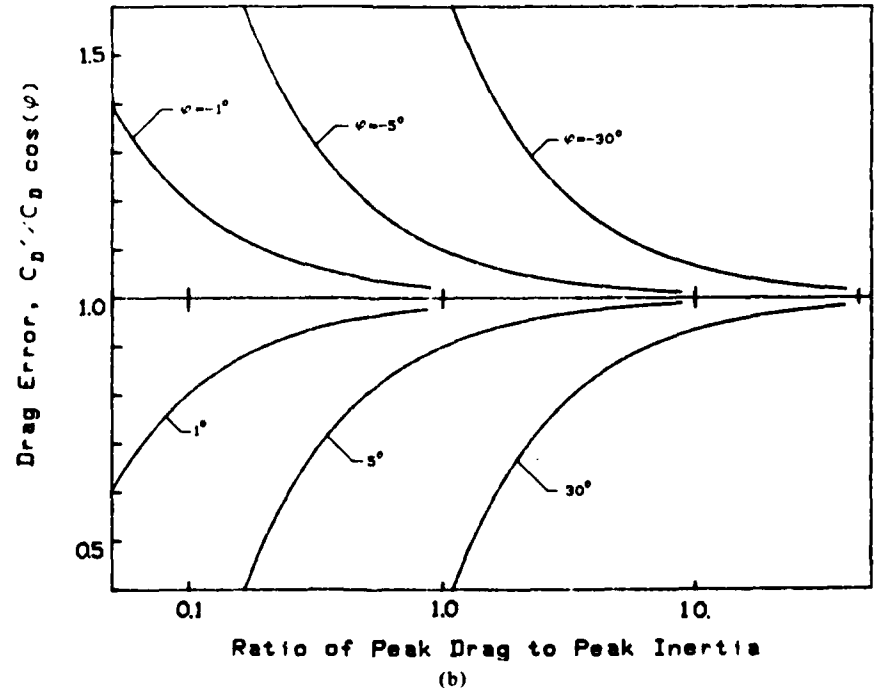

(b)

Figure 3 — The variations in computed force transfer coefficients C_M and C_D as a function of an error in phase between the fluid motion cycle and the force cycle.

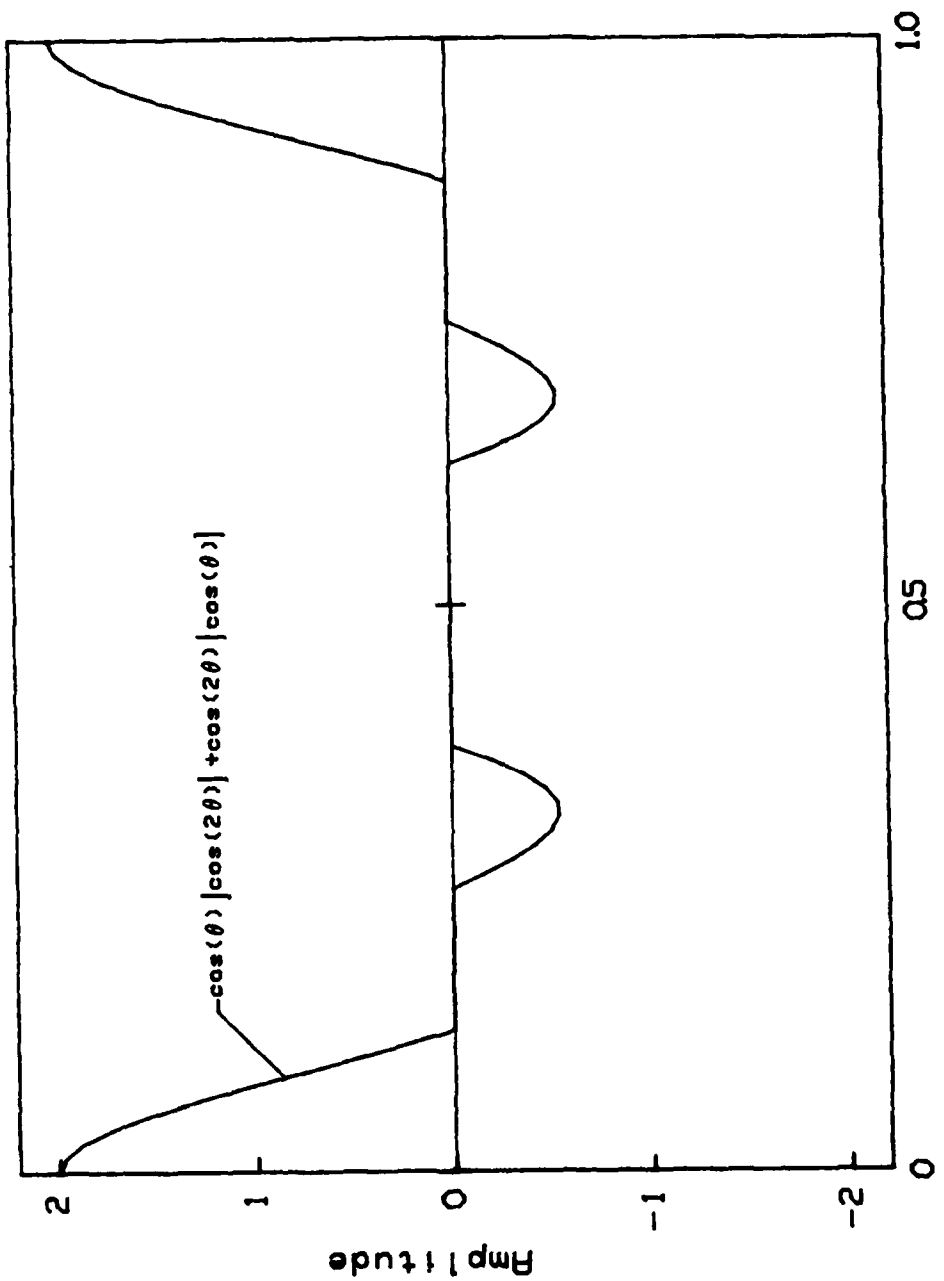

Figure 4 — Harmonic contributions to the predicted Morison drag force due to 2nd order Stokes expansion for the wave kinematics.

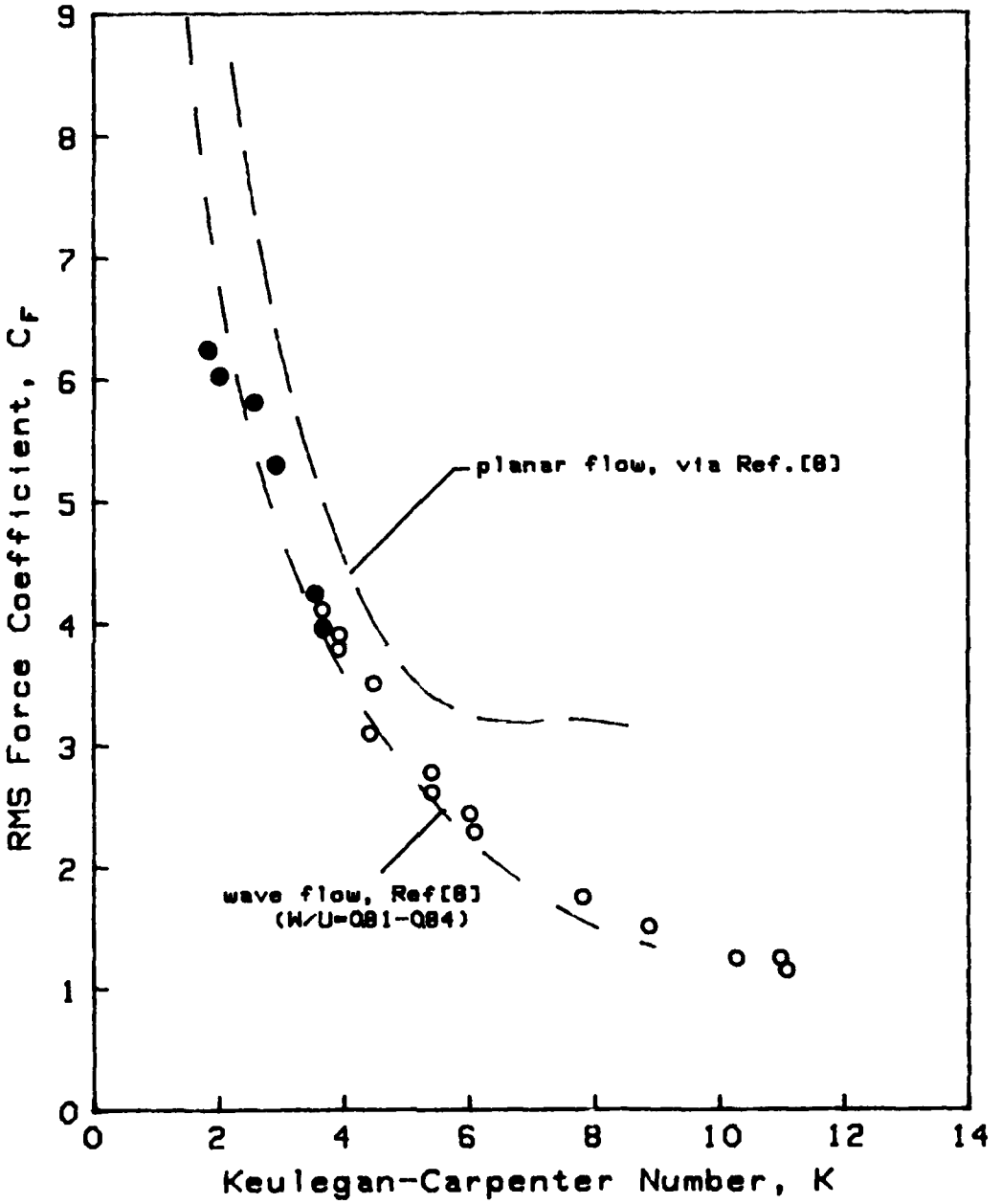

Figure 5 — The in-line RMS wave force coefficients (evaluated for the fundamental frequency) for a horizontal cylinder in waves. Present data: β = 430, ○ β = 610, ●.

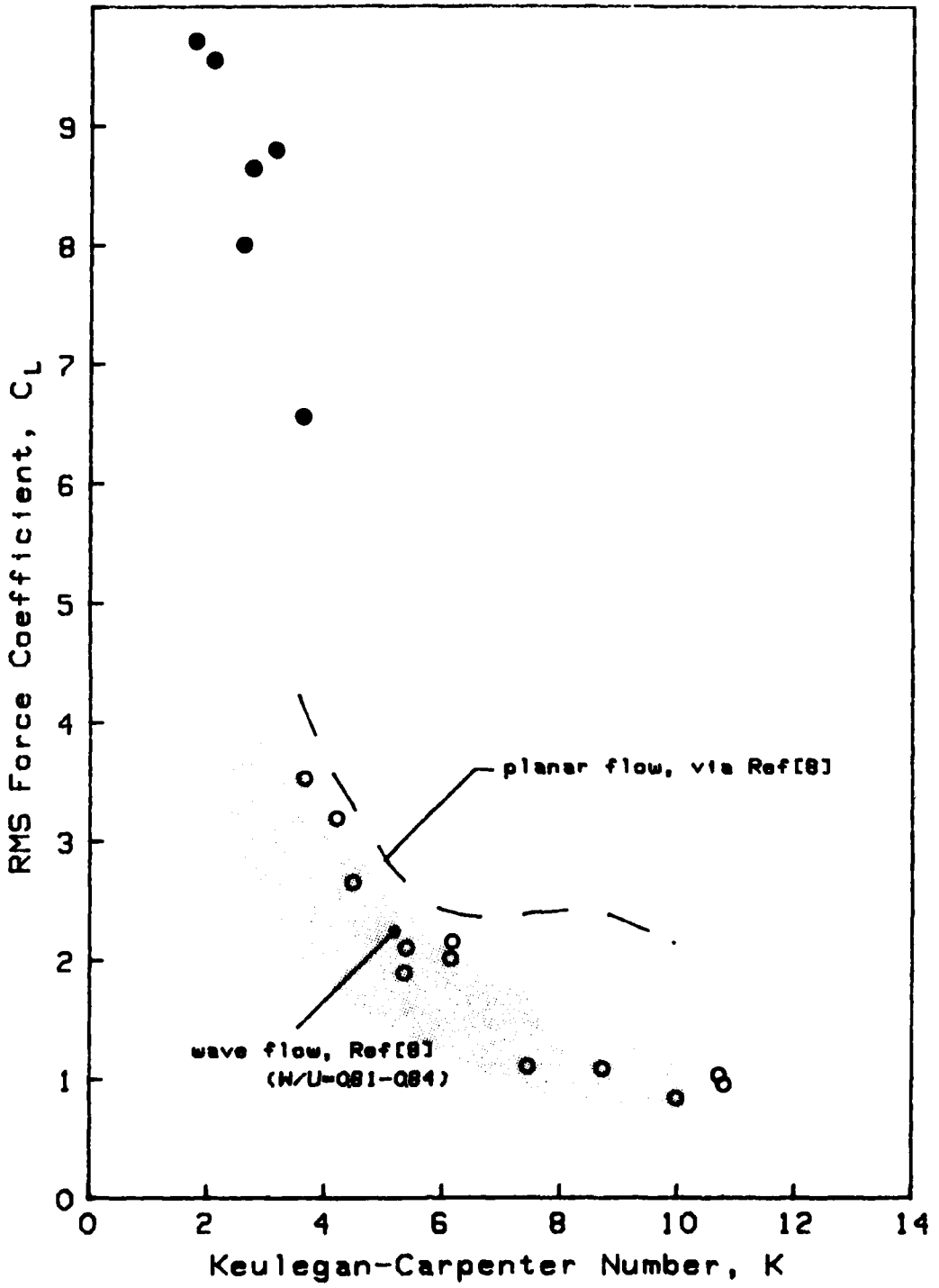

Figure 6 — The transverse RMS wave force coefficients (evaluated for the fundamental frequency) for a horizontal cylinder in waves. Present data: β = 430, ○; β = 610, ●.

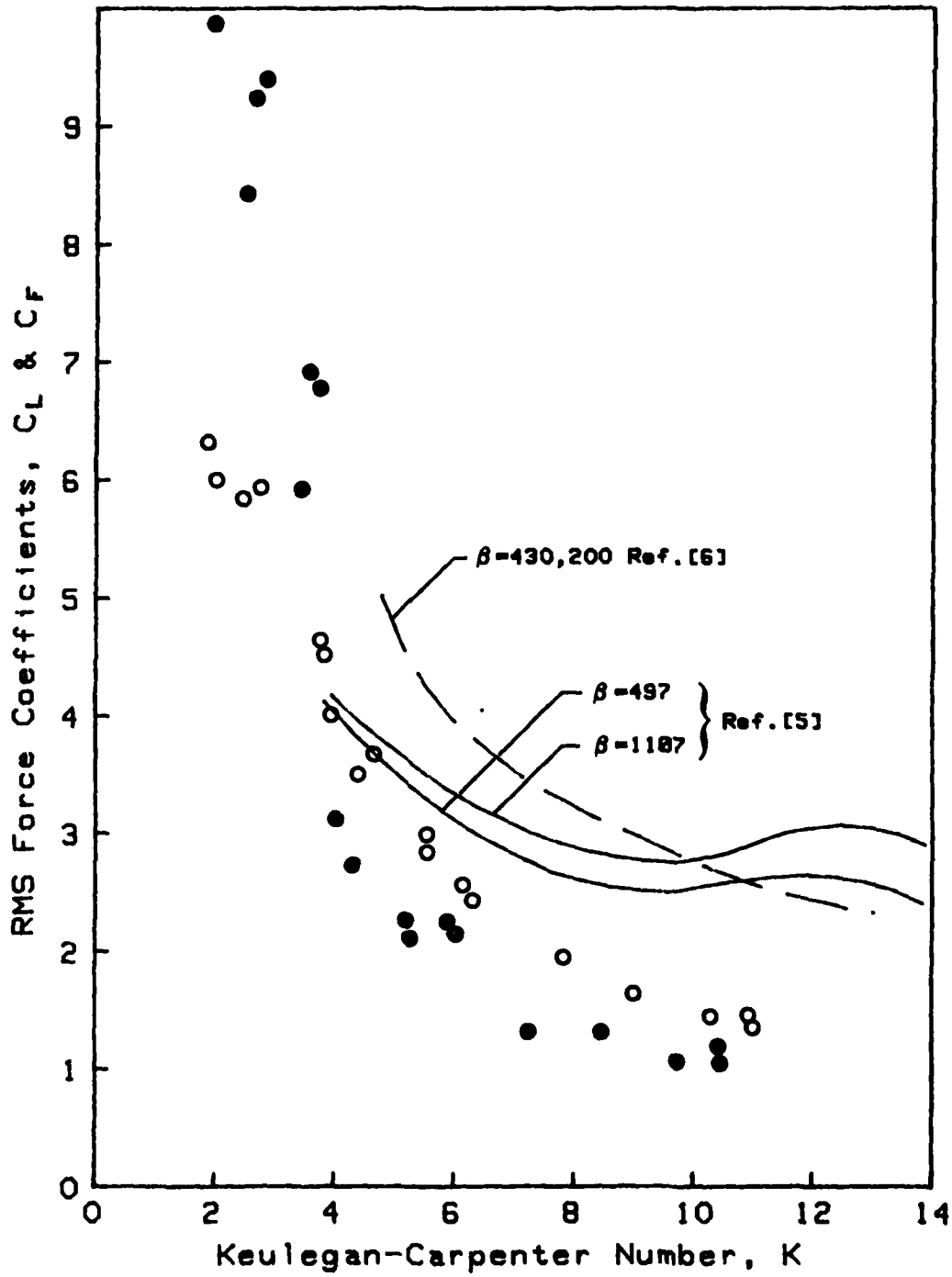

Figure 7 — The total in-line and transverse RMS force coefficients for horizontal cylinders in waves and for corresponding one-dimensional oscillatory flows. Present data: in-line, ○; transverse, ●.

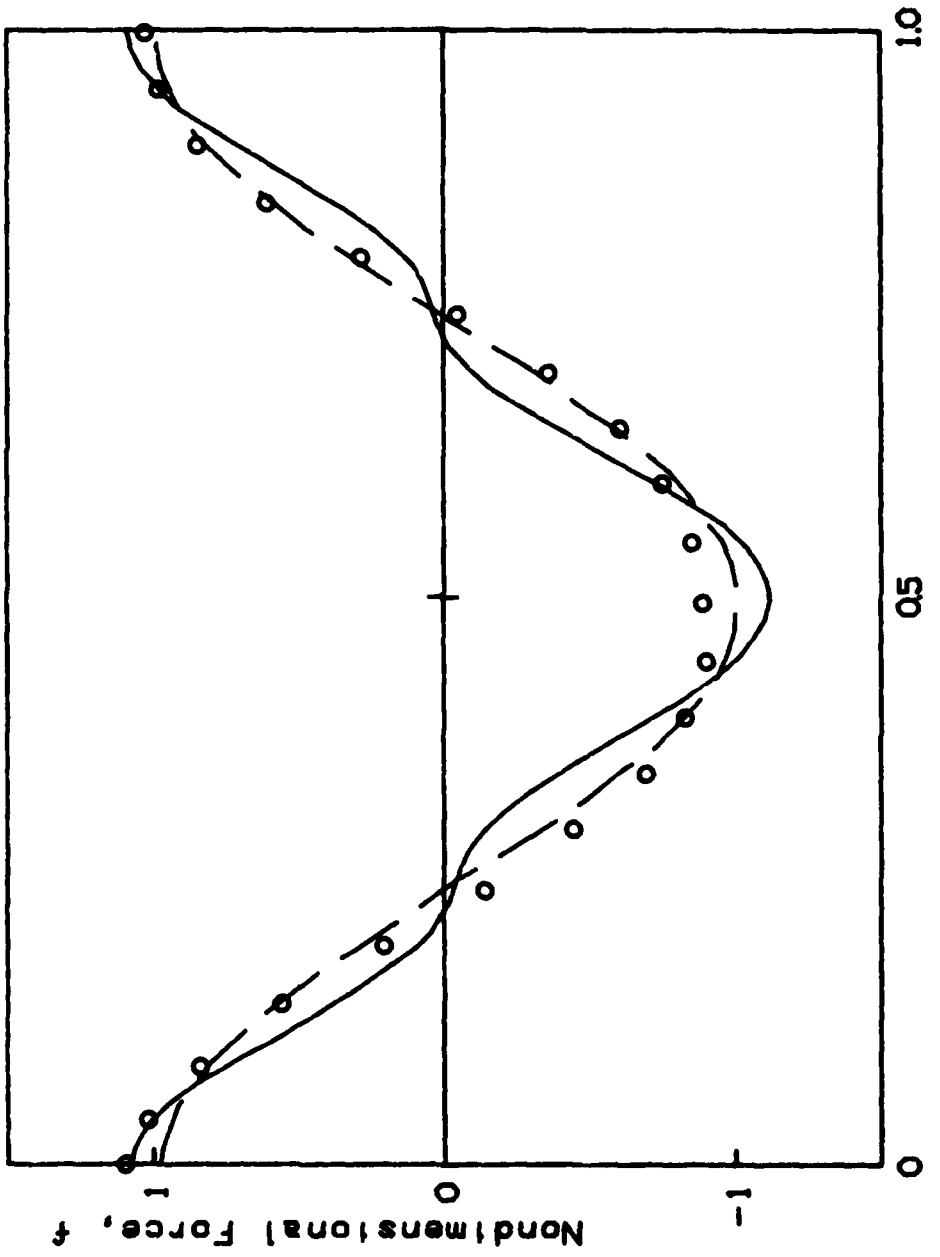

Figure 8 — Two least-squares best fits to a measured wave force on a horizontal cylinder
Usual Morison approach. — (Eqs. 3.13 & 3.14); vector approach. - - - (Eq. 3.15 & 3.16).

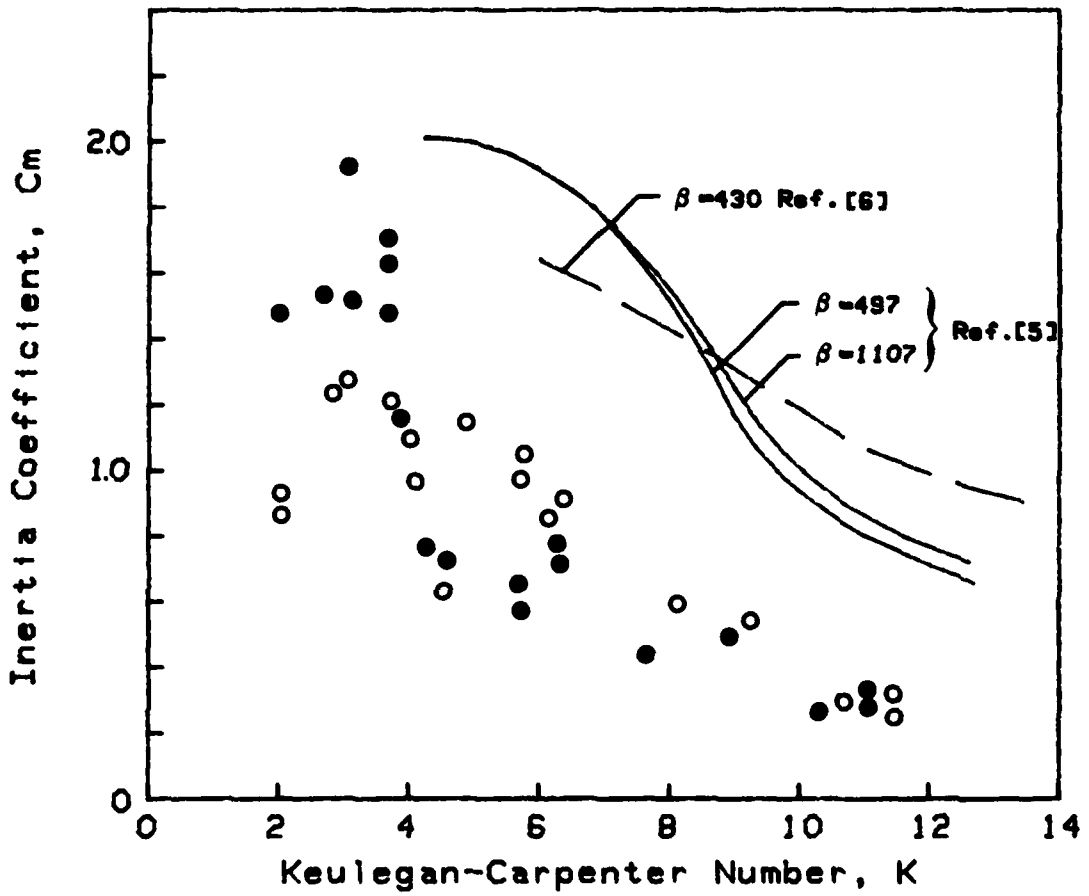

Figure 9 — The in-line and transverse inertia coefficients for horizontal cylinders in waves and for corresponding one-dimensional oscillatory flows. Present data: in-line, ○; transverse, ●.

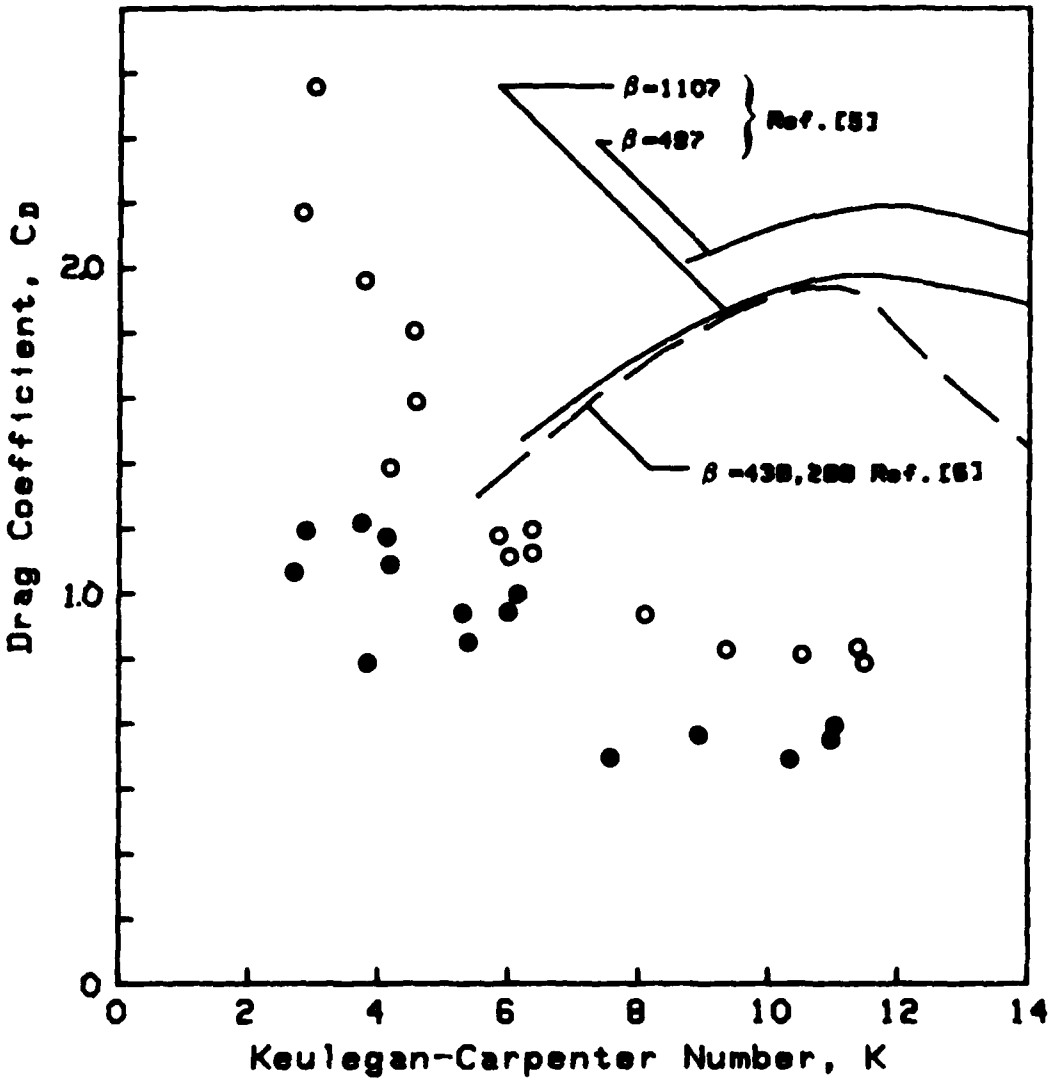

Figure 10 — The in-line and transverse drag coefficients for horizontal cylinders in waves and for corresponding one-dimensional oscillatory flows. Present data, in-line, ○; transverse, ●.

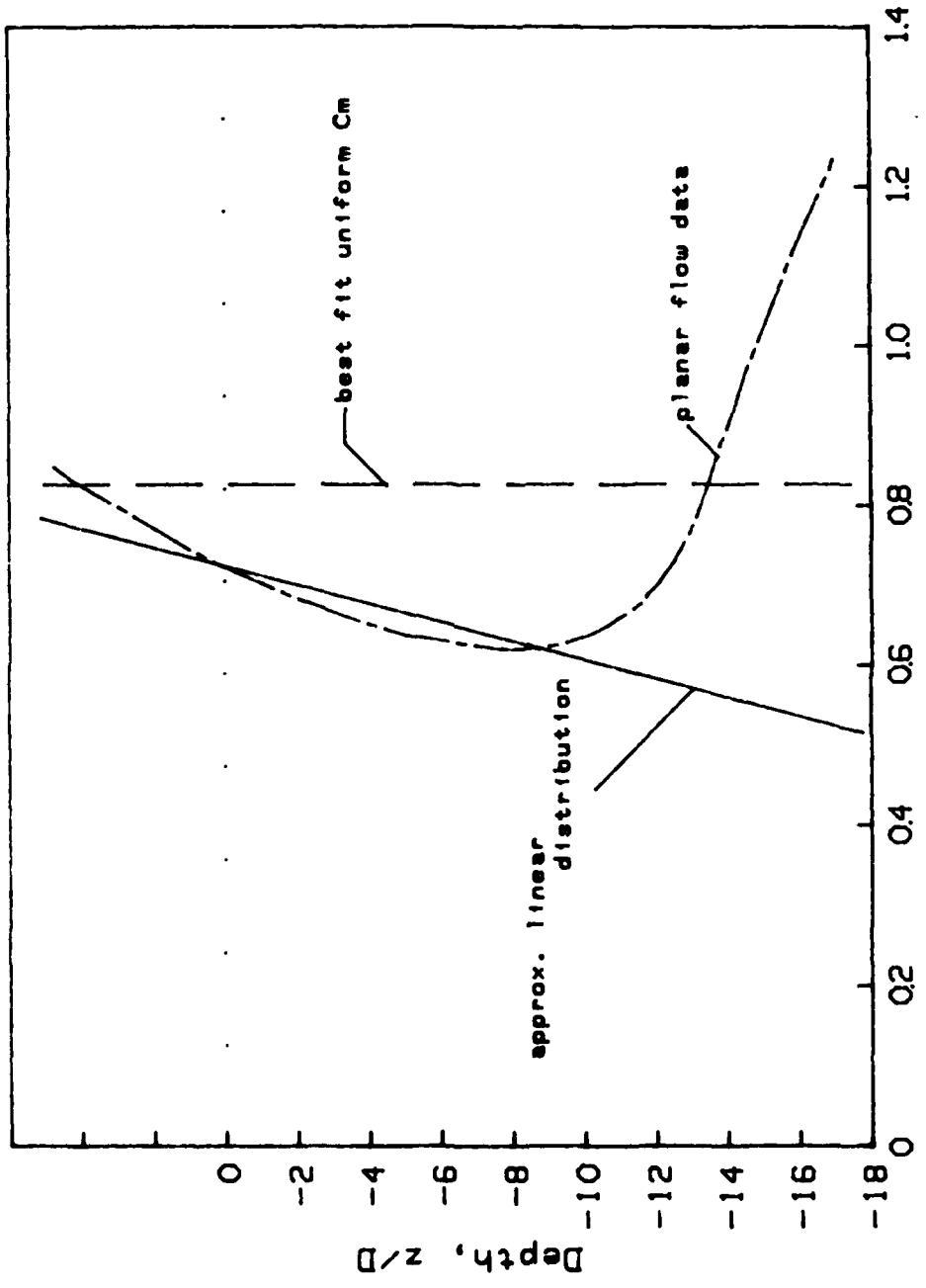

Figure 11 – A comparison between a "best-fit" linear distribution of C_M for a vertical cylinder in waves and a distribution constructed from one-dimensional oscillatory flow results: see Eq. (3.25).

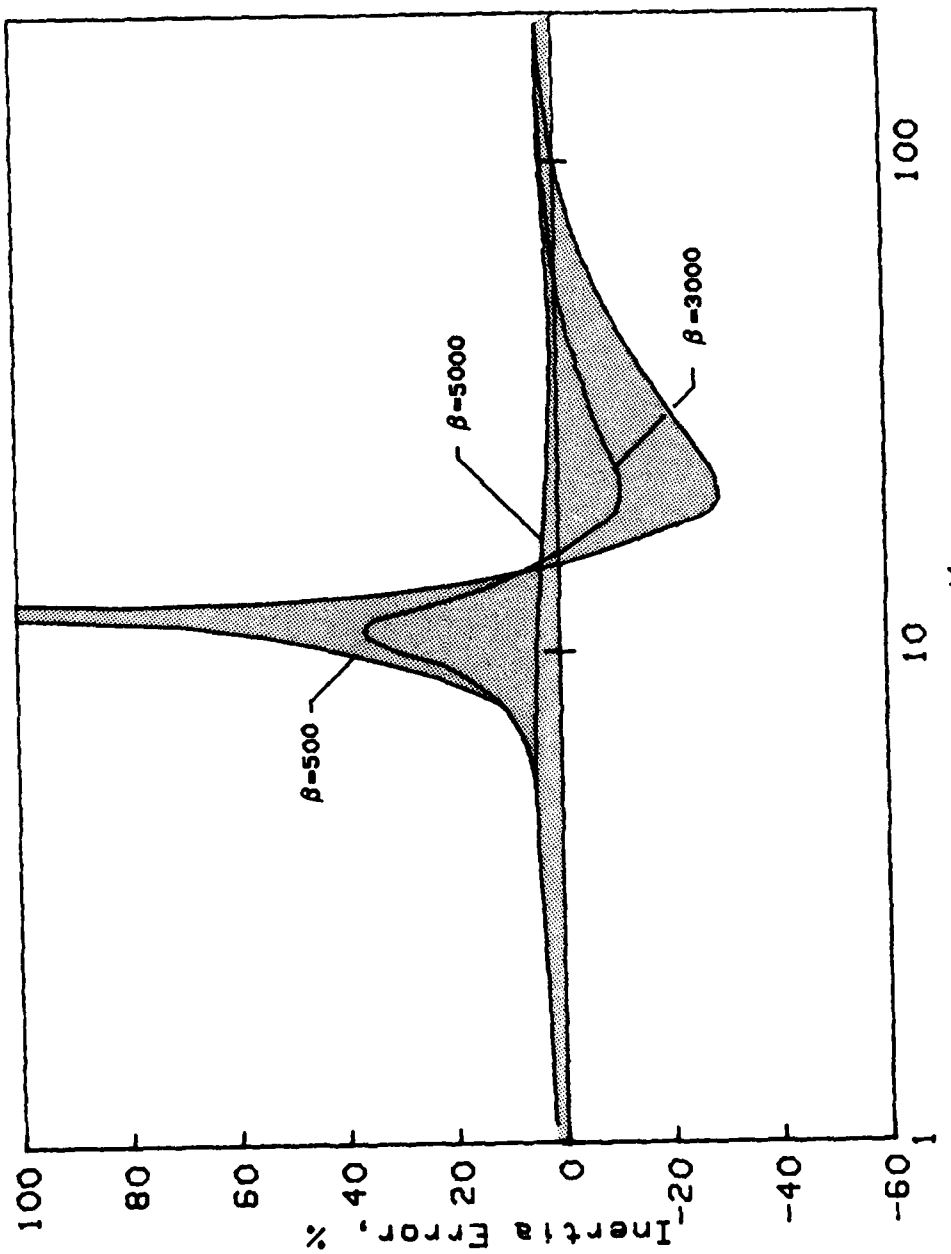

Figure 12 — An estimate of the error in the computed inertia force on a vertical cylinder in deepwater waves when constant, one-dimensional flow values of C_M are employed.

Figure B1 — A photograph of the wave tank.

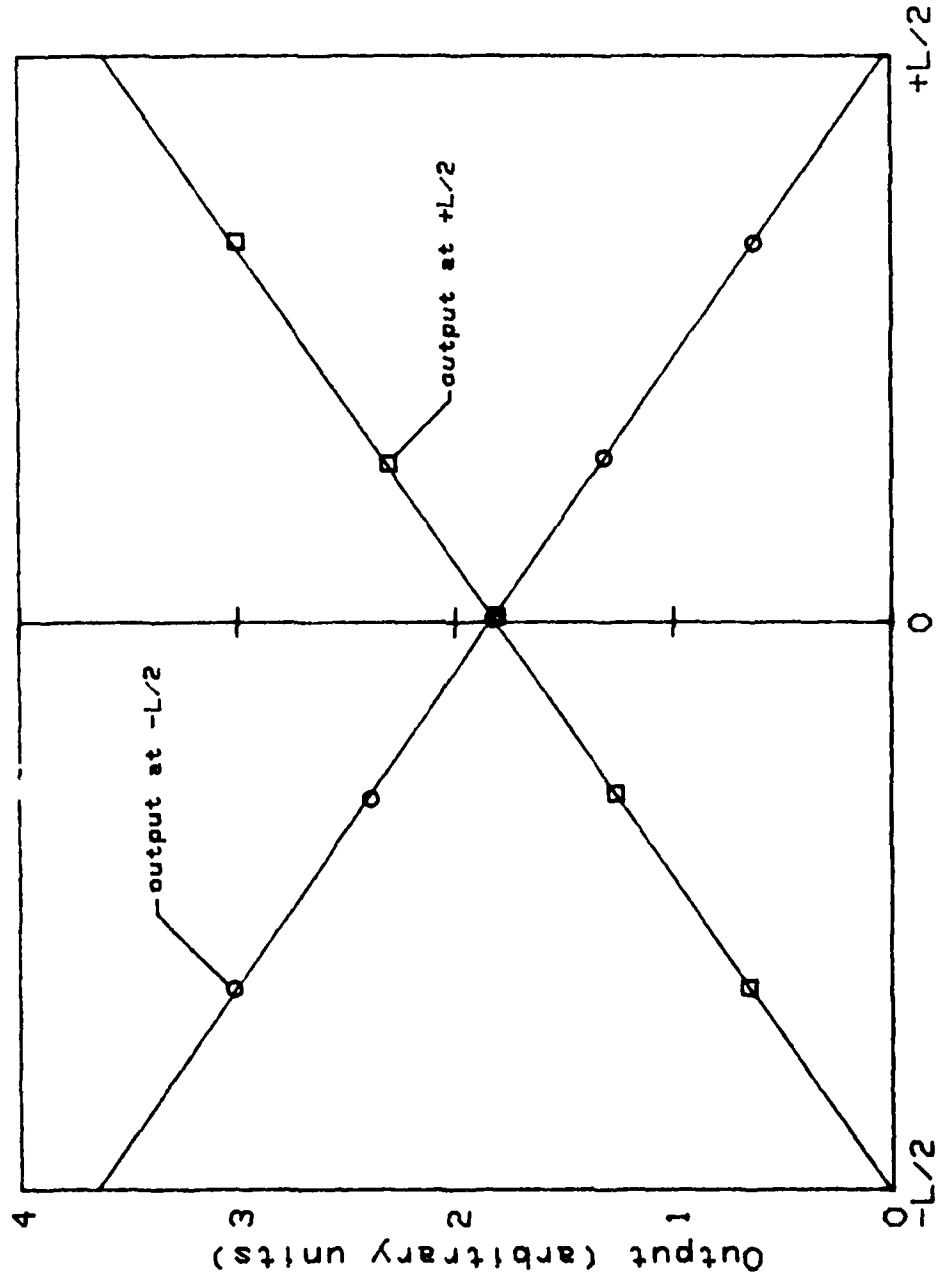

Figure B2 – Force gage outputs as a function of deadweight location along the cylinder span


DAT
FILM